Stem Cell Reports
Article

OPEN ACCESS

Pre-transplantational Control of the Post-transplantational Fate of Human Pluripotent Stem Cell-Derived Cartilage

John Y. Lee,[1,5] Nadine Matthias,[1] Azim Pothiawala,[1] Bryan K. Ang,[1,6] Minjung Lee,[3] Jia Li,[3] Deqiang Sun,[3] Sebastien Pigeot,[4] Ivan Martin,[4] Johnny Huard,[2] Yun Huang,[3] and Naoki Nakayama[1,2,*]

[1]Brown Foundation Institute of Molecular Medicine, The University of Texas Health Science Center at Houston (UTHealth) Medical School, 1825 Pressler St., Houston, TX 77030, USA
[2]Department of Orthopaedic Surgery, UTHealth Medical School, Houston, TX 77030, USA
[3]Institute of Biosciences and Technology, College of Medicine, Texas A&M University, Houston, TX 77030, USA
[4]Department of Biomedicine, University Hospital Basel, Basel CH-4031, Switzerland
[5]Present address: Miller School of Medicine, University of Miami, Miami, FL 33136, USA
[6]Present address: Weill Cornell Medicine, New York, NY 10065, USA
*Correspondence: naoki.nakayama@uth.tmc.edu
https://doi.org/10.1016/j.stemcr.2018.06.021

SUMMARY

Cartilage pellets generated from ectomesenchymal progeny of human pluripotent stem cells (hPSCs) *in vitro* eventually show signs of commitment of chondrocytes to hypertrophic differentiation. When transplanted subcutaneously, most of the surviving pellets were fully mineralized by 8 weeks. In contrast, treatment with the adenylyl cyclase activator, forskolin, *in vitro* resulted in slightly enlarged cartilage pellets containing an increased proportion of proliferating immature chondrocytes that expressed very low levels of hypertrophic/terminally matured chondrocyte-specific genes. Forskolin treatment also enhanced hyaline cartilage formation by reducing type I collagen gene expression and increasing sulfated glycosaminoglycan accumulation in the developed cartilage. Chondrogenic mesoderm from hPSCs and dedifferentiated nasal chondrocytes responded similarly to forskolin. Furthermore, forskolin treatment *in vitro* increased the frequency at which the cartilage pellets maintained unmineralized chondrocytes after subcutaneous transplantation. Thus, the post-transplantational fate of chondrocytes originating from hPSC-derived chondroprogenitors can be controlled during their genesis *in vitro*.

INTRODUCTION

Healthy cartilage of joints is stably maintained, but damaged cartilage is not spontaneously repaired in large animals and humans, leading to severe wear of the whole joint cartilage and consequent osteoarthritis (Buckwalter et al., 2014). The current cell-based and tissue engineering-based therapies, which use mesenchymal stromal cells (MSCs) and dedifferentiated articular chondrocytes, are far from ideal on a number of fronts (Steinert et al., 2007). One of the major challenges is to prevent the (re)generated cartilage from entering an endochondral ossification program after transplantation (Somoza et al., 2014). Such a program results in hypertrophic differentiation, mineralization/calcification, and the death of chondrocytes, followed by angiogenesis and bone growth, as in the growth plate. Similar changes are also observed during osteoarthritic cartilage degeneration (Pitsillides and Beier, 2011; van der Kraan and van den Berg, 2012).

Chondrogenesis is most active during prenatal and early postnatal stages. Surface injury introduced into fetal joint cartilage *in utero* is repaired spontaneously and completely, even in a large animal model (Namba et al., 1998), suggesting that embryonic epiphyseal chondrocytes may possess the capacity to regenerate joint articular cartilage without being committed to endochondral ossification. For humans, pluripotent stem cells (PSCs), including embryonic stem cells (ESCs) and induced PSCs (iPSCs), are the only practical source of embryonic cells. Chondroprogenitors have already been developed from mouse (m) and human (h) PSCs and characterized *in vitro* and *in vivo* (Nakayama et al., 2016; Nakayama and Umeda, 2011). Interestingly, we and others have recently shown that tissue-engineered cartilage produced from mesodermal progeny of hPSCs under scaffold-free conditions *in vitro* (i.e., cartilage pellet) tended to stay in an unmineralized state when transplanted at ectopic sites in immunocompromised rodents (Craft et al., 2015; Umeda et al., 2015; Yamashita et al., 2015), as did a piece of articular cartilage (Figure S1A). This tendency is preserved even when cartilage is formed in the presence of bone morphogenetic protein (BMP) (Umeda et al., 2015; Yamashita et al., 2015), which enhances chondrogenesis but also hypertrophic differentiation of chondrocytes (Minina et al., 2002; Tsumaki et al., 2002). However, when such mesodermal progeny were expanded and maintained in culture, the resulting cartilage pellets matured readily and became fully mineralized after transplantation (Figure S1B). So too did the chondrogenic ectomesenchymal cells developed by an expansion culture of neural crest-like progeny of hPSCs (Umeda et al., 2015). Thus, regardless of the developmental origin, expanded chondroprogenitors may have a tendency to give rise to growth-plate-like, endochondral ossification-ready chondrocytes. However, expansion of chondrogenic cells such

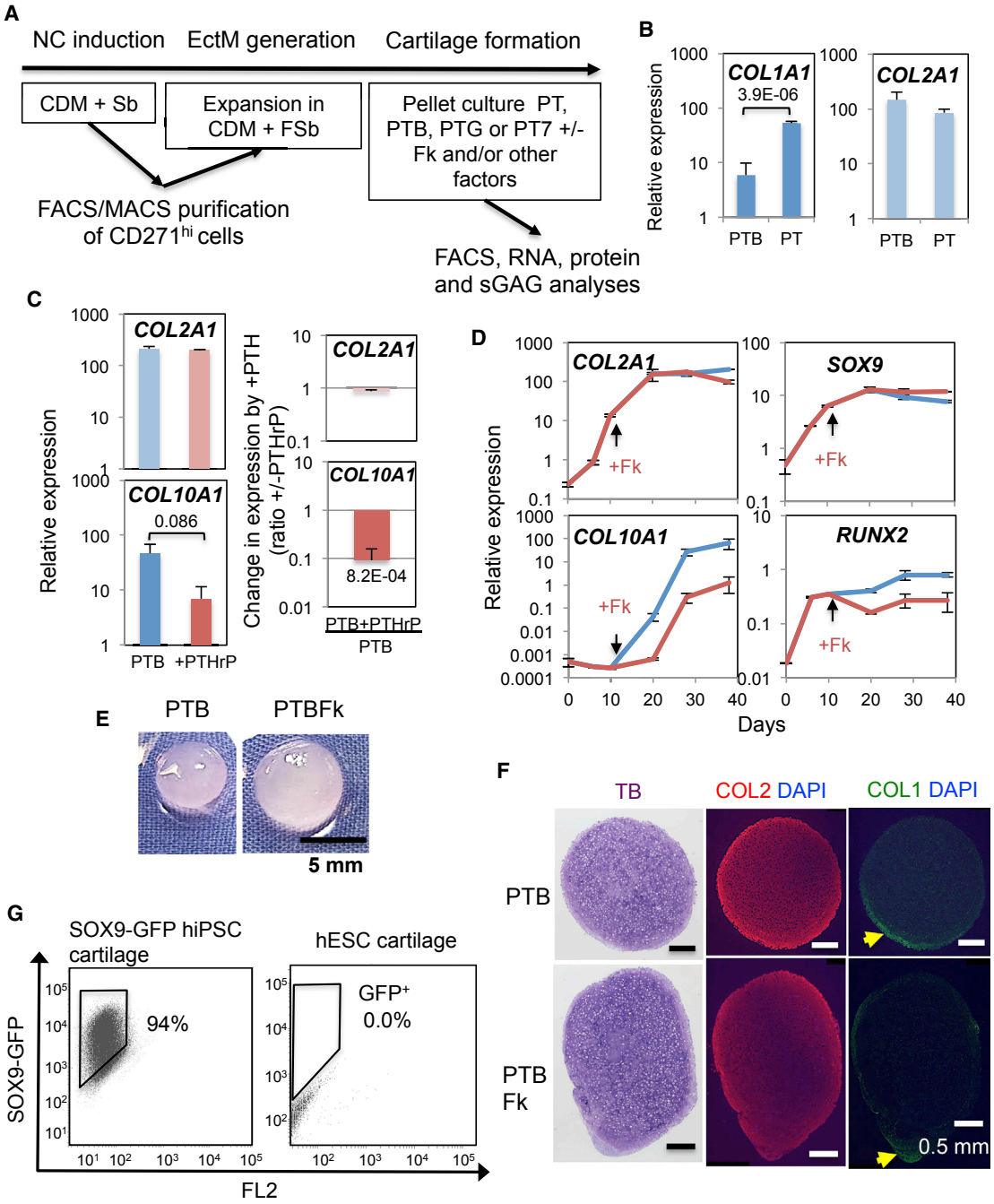

Figure 1. Suppression of Hypertrophic Chondrocyte Gene Expression during Chondrogenesis from hESC-derived Ectomesenchymal Cells

(A) Graphical representation of the experimental procedure. CDM, chemically defined medium; F, FGF2; Sb, SB431542; PT, PDGF + TGF-β; PTB, PT + BMP4; PTG, PT + GDF5; PT7, PT + BMP7.

(B) BMP4 suppression of COL1 gene (*COL1A1*) expression during chondrogenesis. Mean relative expression levels from n = 5–9 (PTB) and n = 6 (PT) are shown with SEM as thin vertical lines and p value.

(C) PTHrP suppression of *COL10A1* expression without affecting *COL2A1* expression. Mean value from n = 4 with SEM and p value. Right: Fold changes in expression by PTHrP treatment. Mean value of the "expression in PTHrP-treated pellets divided by that in untreated pellets" with SEM and p value.

(legend continued on next page)

as MSCs is often needed to gain sufficient cells for treatment.

One way to avoid endochondral ossification in chondrocytes developed from expanded chondroprogenitors is to mimic the parathyroid hormone-related peptide (PTHrP) signaling that keeps growth-plate chondrocytes in the proliferative state and suppresses their hypertrophic differentiation (Amizuka et al., 1994; Karaplis et al., 1994). During embryonic skeletogenesis, early epiphyseal chondrocytes express PTHrP and low levels of its receptor. Later, the Indian hedgehog (IHH)-PTHrP negative feedback loop controls the speed of hypertrophic differentiation and terminal maturation of growth-plate chondrocytes (Lanske et al., 1996; Vortkamp et al., 1996). Increased cAMP is responsible for such effects of PTHrP (Sakamoto et al., 2005). The rise in cAMP leads to activation of Sox9, the master regulator of (immature) chondrocytes, through the action of cAMP-dependent protein kinase (PKA) (Huang et al., 2001, 2000), which also leads to inhibition of Mef2c action and suppression of chondrocyte hypertrophic differentiation (Kozhemyakina et al., 2009). PTHrP causes a decrease in the mRNA level of *Runx2*, the master regulator for mineralization (bone formation) and hypertrophic differentiation of chondrocytes (Li et al., 2004), and stimulates degradation of Runx2 protein (Zhang et al., 2009), which delays chondrocyte hypertrophic differentiation (Guo et al., 2006). Furthermore, *Pthrp* mutant mice show mineralization of nasal cartilage (Chen et al., 2008), suggesting that nasal cartilage is maintained permanently in an unmineralized state via PTHrP signaling.

Here, we report that treatment with the small-molecule activator of adenylyl cyclase forskolin, which directly increases intracellular cAMP levels during chondrogenesis from hPSC-derived ectomesenchymal cells, suppresses hypertrophic differentiation and terminal maturation of developed chondrocytes potentially via maintaining their proliferative state. Forskolin also increases their capacity to produce hyaline cartilage matrix. Furthermore, forskolin treatment prevents cartilage pellets to varying degrees from becoming mineralized bony tissues when transplanted at an ectopic site in immunocompromised mice. Thus, the implementation of cAMP signaling seems to be an effective means of generating a long-lasting, endochondral ossification-resistant cartilage construct.

RESULTS

Forskolin Selectively Suppresses Type X Collagen Gene Expression in Hyaline-like Cartilage Pellets Induced with BMP4 from hPSC-Derived Ectomesenchymal Cells

We used ectomesenchymal cells (Figure 1A) as a model hPSC-derived chondroprogenitor that forms large hyaline-like cartilage (i.e., type I collagen $[COL1]^{lo}$, type II collagen $[COL2]^{+}$) pellets in the presence of BMP (Figures 1B and 1E) (Umeda et al., 2012) and expresses type X collagen (COL10) mRNA (*COL10A1*), a marker of hypertrophic chondrocytes (Figures 1C and 1D) (Umeda et al., 2015) to screen for signaling modifiers that counteract the effect of BMP on hypertrophic differentiation of chondrocytes without disturbing its effect on hyaline chondrogenesis *in vitro*. We aimed to manipulate signaling mechanisms of canonical WNT (stabilizing β-catenin), PTHrP (increasing cAMP), and natriuretic peptide (NP, increasing cGMP). WNT and NP promote, and PTHrP antagonizes, hypertrophic differentiation of chondrocytes in the growth plate (Nakayama et al., 2016).

We first tested the effect of PTHrP directly (Figure 1C). Addition of PTHrP(1–34) peptide enhanced the growth of cartilage pellets and suppressed *COL10A1* expression without affecting COL2 mRNA (*COL2A1*) levels during chondrogenesis in the standard medium (PTB), which includes platelet-derived growth factor (PDGF), transforming growth factor (TGF) β3, and BMP4 (Umeda et al., 2012, 2015). During chondrogenesis, *COL2A1* expression was stimulated by TGF-β added from day 6 until the levels plateaued around days 20–30, whereas *COL10A1* expression became detectable after BMP4 treatment initiated on day 10 (Figure 1D). Accordingly, to restrict its effect on the BMP-promoted chondrocyte hypertrophic differentiation, we added PTHrP on days 11–12, when $COL2A1^{+}COL10A1^{-}$ immature chondrocytes were being made and BMP signal had just begun.

We further investigated small molecules known to directly elevate cAMP (forskolin), to inhibit canonical WNT signaling (iCRT14 and KY02111), to inhibit all WNT signaling (Verapamil and Wnt-C59), or to inhibit cGMP signaling (KT5824) (Figures S2A–S2C). Initial screening demonstrated that forskolin strongly suppressed

(D) Time-dependent changes in gene expression during chondrogenesis under PTB with (brown) or without (blue) forskolin (Fk) treatment (n = 2). Thin vertical line, SD.

(E) Translucent cartilage pellet formation from H9 hESC-derived ectomesenchymal cells under PTB with or without Fk.

(F) Histological and immunofluorescence staining of the cartilage pellet formed as in (E). Representative results of n = 3. TB, toluidine blue. The yellow arrow indicates the $COL1^{+}$ area.

(G) Composition of $SOX9^{+}$ chondrocytes within the cartilage pellets formed under PTBFk from SOX9-GFP hiPSC-derived ectomesenchymal cells (left), analyzed by fluorescence-activated cell sorting (FACS). Those derived from H9 hESCs were used for the non-GFP control (right). Representative results of n = 8. Gene expression data are provided in Figure S3C.

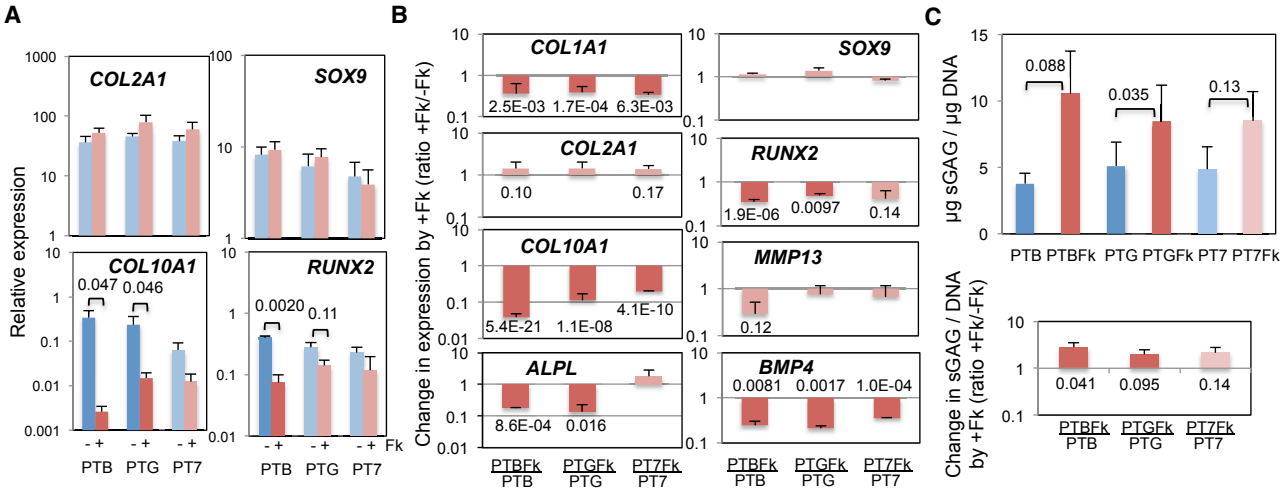

Figure 2. Effect of Different BMPs on the Forskolin Suppression of Hypertrophic Chondrocyte Gene Expression and Forskolin Enhancement of Sulfated Glycosaminoglycan Production

(A) Effect of replacement of BMP4 in PTB (PDGF + TGF-β+BMP4) with GDF5 (PTG) or BMP7 (PT7) on gene expression during chondrogenesis with (brown) or without (blue) forskolin (Fk). Mean relative expression levels from n = 3–5 (*COL2A1*), 3–6 (*SOX9* and *COL10A1*), and 3 (*RUNX2*) with SEM and p values. Additional data are provided in Figure S3A.

(B) Fold changes in expression by Fk addition. Mean values from n = 3–12 shown with SEM and p values. Table S7 shows all n and p values.

(C) Quantitative comparison of the capacity of chondrocytes generated under PTB, PTG, and PT7 with (brown) or without (blue) Fk to produce sulfated glycosaminoglycan (sGAG). Top: Mean values of µg sGAG/µg DNA (n = 4–5) shown with SEM and p values. Bottom: Mean fold changes in the µg sGAG/µg DNA values by Fk treatment with SEM and p values (n = 4).

(Figure S2A), and Wnt-C59 weakly suppressed (Figure S2C), the expression of *COL10A1*, without significantly affecting *COL2A1* expression and growth of the cartilage pellet. Other agents failed to show a significant effect on *COL10A1* expression and were somewhat inhibitory to the growth of cartilage pellets.

Therefore, we focused on cAMP signaling activated by forskolin for further analysis. Forskolin added at 20–30 µM (Figure S2D) during chondrogenesis under PTB reproducibly decreased and delayed the expression of *COL10A1* and to a lesser degree *RUNX2* (one of the critical *COL10A1* transcription factors), without affecting the level and kinetics of expression of the chondrocyte genes *COL2A1* and *SOX9* (the major *COL2A1* transcription factor) (Figure 1D). Immunohistological analysis showed that uniform metachromatic staining by toluidine blue (TB; i.e., uniform sulfated glycosaminoglycan [sGAG] accumulation) overlapped with COL2 immunostaining within the cartilage pellet but that COL1 was only detectable in the layer of cells at the periphery of pellets, more so in those formed without forskolin (Figure 1F). In support, the forskolin-treated cartilage pellets consisted mostly of $SOX9^+$ chondrocytes, assessed as the proportion of GFP^+ cells in cartilage generated from SOX9-GFP hiPSC-derived ectomesenchymal cells (mean % $SOX9\text{-}GFP^+$ cells, 82.9 ± 11.7 [SEM]; Figure 1G). Thus, although forskolin and PTHrP(1–34) can be inhibitory for chondrogenesis from MSCs (Fischer et al., 2014), no sign of inhibition of chondrogenesis was observed in the hPSC-derived ectomesenchymal cells.

The Suppression of Hypertrophic Chondrocyte Gene Expression and Enhancement of Sulfated Glycosaminoglycan Production by Forskolin Are Not Affected by the Type of BMP Used

GDF5 and BMP7, members of the BMP family, are known to support chondrocyte hypertrophic differentiation only weakly (Caron et al., 2013; Enochson et al., 2014; Hatakeyama et al., 2004). However, under PTG or PT7 conditions, in which BMP4 in PTB is replaced with GDF5 or BMP7, respectively, the expression of *COL10A1* and *RUNX2* was induced during chondrogenesis to levels not significantly different from those under PTB (blue; Figure 2A). In contrast, forskolin treatment suppressed the expression of both genes (brown): e.g., expression of *COL10A1* was suppressed by 98% in PTB (from the relative expression of 0.25 to 0.0045) and 94% in PTG (from 0.26 to 0.015), while that of *COL2A1* and *SOX9* was not significantly affected. Changes in the expression of individual genes by forskolin treatment (+Fk) are summarized in Figure 2B, which shows the +Fk expression level normalized by the corresponding −Fk level

(where −Fk = 1). Among hypertrophy genes, forskolin suppression of *COL10A1* expression was statistically significant in all BMP types tested. For the alkaline phosphatase gene (*ALPL*) and *RUNX2*, reproducible suppression was observed under PTB and PTG but not under PT7 conditions. Forskolin effects on *MMP13* expression were not significant under any of the BMP conditions tested. As expected, changes of the (immature) chondrocyte genes, *COL2A1* and *SOX9*, were weak and statistically insignificant. However, expression of *COL1A1* was significantly reduced by forskolin (Figures 2B and S3A), suggesting that it may enhance hyaline chondrogenesis. Forskolin treatment also significantly reduced mRNA levels of *BMP4* in all BMP conditions.

A high level of sGAG is a key indicator of healthy articular cartilage. Therefore, we investigated the effect of forskolin on sGAG accumulation in cartilage pellets. Under both PTB and PTG conditions, forskolin treatment resulted in a significant increase in the capacity of chondrocytes to produce sGAG (Figure 2C). The PT7 condition showed the same tendency but with only a weak statistical significance. Thus, forskolin supports hyaline cartilage formation by suppressing *COL1A1* expression and stimulating sGAG production from chondrocytes, consistent with a previous suggestion (Malemud et al., 1986), regardless of the type of BMPs used.

Exogenous cAMP Replaces Forskolin to Suppress *COL10A1* Expression during Chondrogenesis

Next, we set out to confirm that the suppressive effect of forskolin on *COL10A1* gene expression during chondrogenesis is dependent on the cAMP signaling pathways: i.e., one through PKA and/or another through the exchange protein directly activated by cAMP (EPAC) (Beckler et al., 2011). We tested the effects of the cAMP analogs N^6-benzoyl cAMP (Bnz-cAMP) and 8-pCPT-2′-O-Me-cAMP-AM (CPT-cAMP), which preferentially bind and activate PKA and EPAC, respectively (Christensen et al., 2003; Poppe et al., 2008). We also tested the effect of IBMX, an inhibitor of phosphodiesterase, the enzyme that degrades cAMP and cGMP. The PKA-activating Bnz-cAMP significantly inhibited *COL10A1* expression during chondrogenesis under PTB (+cAMP; Figures 3A and 3B) in a dose-dependent manner (Figure S4A). IBMX at 0.5 mM also significantly reduced the *COL10A1* levels (+IBMX). These treatments had no significant effect on the level of *COL2A1* expression (Figures 3A and 3B). In contrast, the EPAC-activating CPT-cAMP reduced the *COL10A1* levels, albeit to a much smaller degree (Figure S4A), and the cGMP antagonist Rp-8-Br-PET-cGMPS had no effect on *COL10A1* (Figure S4B). These results suggest that suppression by forskolin of *COL10A1* expression during chondrogenesis involves the cAMP-PKA pathway.

Effect of Porcupine Inhibitor on the Forskolin-Dependent Decrease in *COL10A1* Expression during Chondrogenesis

Even in the presence of forskolin, *COL10A1* expression was induced, albeit slowly (only after day 20) and weakly (brown; Figure 1D), resulting in low but variable levels of background expression by day 28 of chondrogenesis (i.e., relative expression of *COL10A1* of between 0.0045 and 0.012; Figure 2A). We hypothesized that the hypertrophy-inducing canonical WNT signaling might contribute to such background expression. The weak (<50%) inhibitory effect of Wnt-C59 (Figure S2C) on *COL10A1* gene expression observed in the initial screening was reproducible (Figure 3B), consistent with Narcisi et al. (2015). However, addition of Wnt-C59 with forskolin did not significantly enhance the inhibition of *COL10A1* expression due to forskolin alone (Figure 3B). Therefore, the residual expression of *COL10A1* in forskolin-treated cartilage pellets was probably not supported by endogenous WNT signaling.

Forskolin Promotes Accumulation of Proliferating Chondrocytes within Cartilage Pellets

Forskolin-treated cartilage may maintain *COL2A1*$^+$ *COL10A1*^{lo} hyaline chondrocytes either by blocking their hypertrophic differentiation or by supporting their proliferation and survival. PTHrP is known to maintain immature chondrocytes in a proliferative state in growth plate (Amizuka et al., 1994; Karaplis et al., 1994). Since forskolin treatment caused a slight enlargement of cartilage pellets (1.31 ± 0.089 [SEM] fold increase in diameter, n = 7, p = 6.2E−04; Figure 1E), we tested whether forskolin mimicked the proliferative effect of PTHrP by immunostaining 30-day-old cartilage pellets with antibodies for Ki67, the protein marker for cell proliferation, and COL2. Forskolin treatment led to a significant increase in the proportion of chondrocytes expressing Ki67 in the cartilage pellets produced under PTB (indicated by the ratio of Ki67$^+$ nuclei/DAPI$^+$ nuclei in the COL2$^+$ area; Figure 3C), although cartilage pellets formed under PTG and PT failed to show statistically significant differences (Figure S4C). Next, we conducted a 5-ethynyl-2′-deoxyuridine (EdU) incorporation study on day 26–28 cartilage pellets. The study demonstrated that addition of forskolin significantly increased the proportion of DNA-replicated chondrocytes (SOX9-GFP$^+$EdU$^+$ cells) within the cartilage pellets formed under PTB from SOX9-GFP hiPSC-derived ectomesenchymal cells (Figures 3D, S4D, and S4E). These results support our hypothesis that forskolin increases the proportion of immature chondrocytes within the formed cartilage by stimulating chondrocyte proliferation.

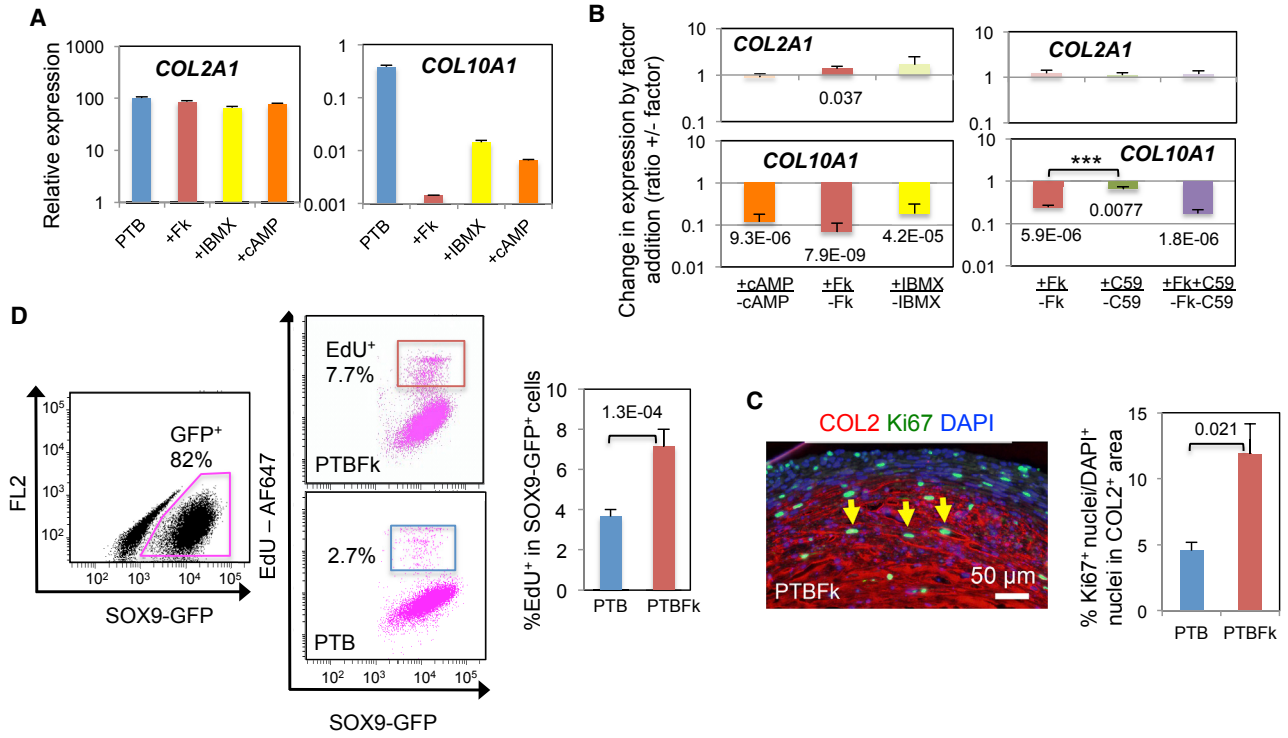

Figure 3. Mechanistic Insight into the Effect of Forskolin on the Formation *In Vitro* of *COL2A1*$^{+}$*COL10A1*^{lo} Cartilage from hESC-Derived Ectomesenchymal Cells

(A) Effects of the cAMP analog, Bnz-cAMP, and PDE-inhibitor, IBMX, on *COL2A1* and *COL10A1* expression during chondrogenesis. Representative results of n = 3–4. Thin vertical line, SD of three technical repeats. cAMP, 80 μM Bnz-cAMP; IBMX, 0.5 mM. Additional data are provided in Figures S4A and S4B.

(B) Mean fold changes in *COL2A1* and *COL10A1* expression by addition of a factor during chondrogenesis under PTB (PDGF + TGF-β + BMP4) are shown with SEM and p values. Table S7 shows all n and p values. Factors: cAMP, 100 μM Bnz-cAMP; IBMX, 0.5 mM; C59, 30 nM Wnt-C59. Changes by +Fk (forskolin) versus +C59: ***p = 0.0031.

(C and D) Quantitation of proliferating chondrocytes within cartilage pellets formed under PTB with or without Fk.

(C) Left: Immunofluorescence image of Ki67 and COL2 staining of a PTBFk pellet. Right: Mean value of the % Ki67^{+} nuclei/total (DAPI^{+}) nuclei of the COL2^{+} area from n = 4 with SEM with p value. The yellow arrow indicates the Ki67^{+} nucleus. Additional data are provided in Figure S4C.

(D) EdU incorporation. Left: EdU labeled chondrocytes formed from the SOX9-GFP hiPSC-derived ectomesenchymal cells under PTB and PTBFk were FACS analyzed. Representative image of n = 4. The pink dot plots represent cells gated with the pink gate (i.e., SOX9-GFP^{+} chondrocytes). Right: Mean % EdU^{+} cells within the SOX9-GFP^{+} cell population are shown with SEM and p value. Additional results are provided in Figures S4D and S4E.

Forskolin Suppresses *COL10A1* Expression without Affecting *COL2A1* Expression during Chondrogenesis in Different Cell Systems

The SOX9-GFP hiPSC-derived ectomesenchymal cells that underwent chondrogenesis under PTB or PTG conditions also showed that the expression of *COL10A1* was selectively decreased by forskolin treatment (Figure S3C). In addition, when chondrogenic paraxial mesoderm was derived from hESCs, expanded in a chemically defined medium (CDM) containing fibroblast growth factor (FGF) 2 and SB431542 and CHIR99021 (FSbC condition; Figure 4A) and subjected to pellet chondrogenesis culture under PTB, we observed a similar selective reduction in the *COL10A1* expression. The levels of *COL2A1* transcript were unchanged (Figures 4B and 4C).

Nasal chondrocytes originate from cranial neural crest (i.e., ectomesenchymal cells). Therefore, adult nasal chondrocytes isolated from three patients were propagated (and inevitably dedifferentiated) and subjected to *in vitro* chondrogenesis as described (Pelttari et al., 2014) (Figures 4D, 4E, and S5A). The low levels of *COL2A1* and *COL10A1* mRNA detected on days 6–9 of differentiation declined to a near undetectable level (relative expression level of 0.001) by day 28 in the presence of TGFβ3 alone (T, green). However, the addition of BMP4 on day 10 stimulated *COL2A1* expression and to a much lesser degree,

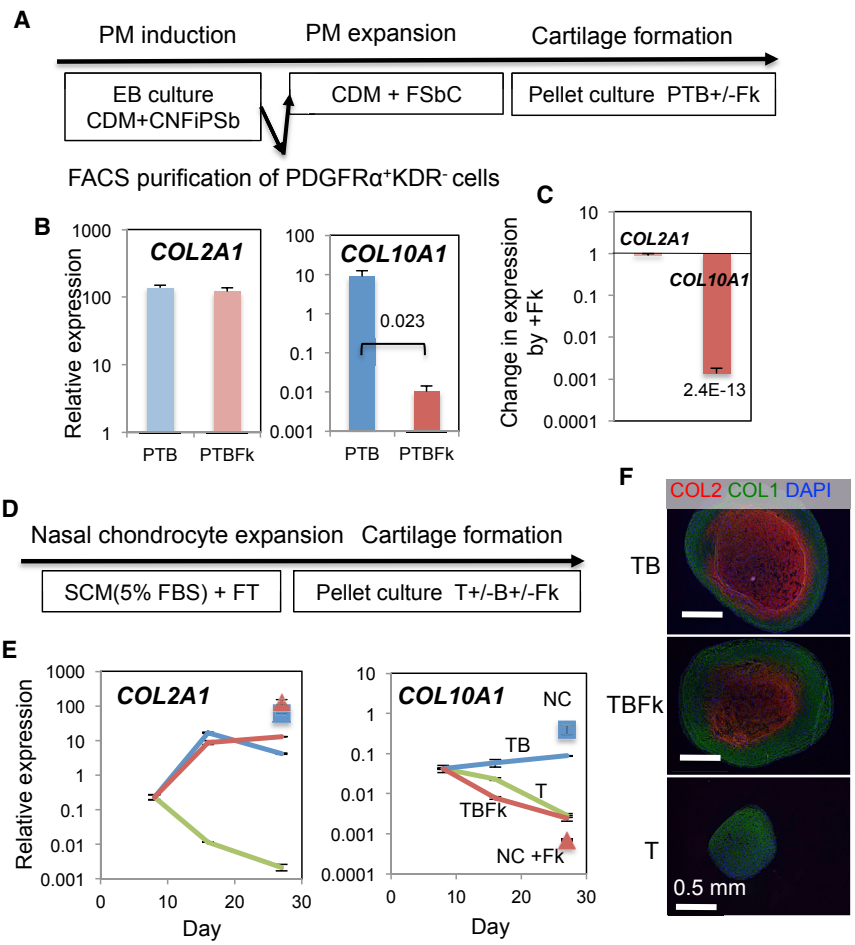

Figure 4. Effects of Forskolin during Chondrogenesis from hESC-derived Paraxial Mesoderm and from Dedifferentiated Human Adult Nasal Chondrocytes

(A) Graphical representation of the experimental procedure for developing chondrogenic paraxial mesoderm (PM). C, CHIR; N, Noggin; Fi, PD173074; P, PDGF; Sb, SB431542; T, TGFβ3; B, BMP4.

(B and C) Mean relative expression levels of *COL2A1* and *COL10A1* in cartilage pellets formed under PTB and PTB with forskolin (PTBFk) (B), and mean fold changes in expression of *COL2A1* and *COL10A1* by Fk treatment (C) are shown with SEM and p value (n = 5).

(D) Graphical representation of the experimental procedure for human nasal chondrocytes. SCM, serum-containing medium; FBS, fetal bovine serum.

(E) *COL2A1* and *COL10A1* expression during chondrogenesis under T (green) and TB conditions with (TBFk, brown) or without (TB, blue) Fk. Square, cartilage from hESC-ectomesenchymal cells formed under PTB (NC); triangle, cartilage formed under PTBFk (NC + Fk). Thin vertical line, SD of three technical repeats. Results from two other patient samples are shown in Figure S5A.

(F) Immunofluorescence images of the cartilage pellets generated under T, TB, and TBFk conditions. Toluidine blue staining for sGAG is shown in Figure S5B.

COL10A1 expression (TB, blue). The addition of forskolin (TBFk, brown) on day 12 selectively knocked down the BMP4-supported *COL10A1* expression without affecting the BMP4-enhanced *COL2A1* expression. Furthermore, immunohistological analyses supported the finding that in nasal cartilage pellets, the accumulation of COL2 (Figure 4F) and sGAG (Figure S5B) was dependent on BMP4 and independent of forskolin.

Thus, chondrogenesis from human neural-crest-derived ectomesenchymal cells, human paraxial mesoderm-derived chondroprogenitors, and dedifferentiated adult human nasal chondrocytes is sensitive to forskolin treatment, which leads to the suppression of the BMP-stimulated commitment of the developed chondrocytes to hypertrophic differentiation without affecting the enhancement of chondrogenesis by BMP.

Forskolin Treatment Maintains the Expression of Genes Representing "Proliferative" and "Primitive" Stages of Chondrocytes

To elucidate the type of cartilage that forskolin forms preferentially and the potential molecular mechanisms involved in the process, we performed genome-wide, comparative transcriptome analyses on the cartilage pellets formed from three to four independent pellet cultures of ectomesenchymal cells under PTB conditions with or without forskolin treatment. RNAs were isolated on day 26–28 and mRNA-sequencing analyses were performed. The principal component analysis and heatmap demonstrated that forskolin-treated cartilage pellets were distinct from forskolin-untreated cartilage pellets (Figures 5A and 5B). Gene ontology (GO) analysis on differentially expressed genes (DEGs, genes showing more than a 2-fold difference in the expression level between forskolin-treated and untreated pellets; Tables S1 and S2) indicated that forskolin treatment during chondrogenesis would likely enhance "(nuclear) chromosome segregation" in the cells, suggesting the enhancement of the cell division cycle of chondrocytes (Figure 5C, Table S1). In support, the forskolin-induced gene set contained various cell-cycle regulator genes, including *CCNA2/B2*, *CDK1/18*, and *CDC45* (Otto and Sicinski, 2017), and DNA replication genes such as *MCM10*, *ORC1*, and *CDT1* (Sclafani and Holzen, 2007) (Figure 5E, Table S3). Consistently, the forskolin-suppressed

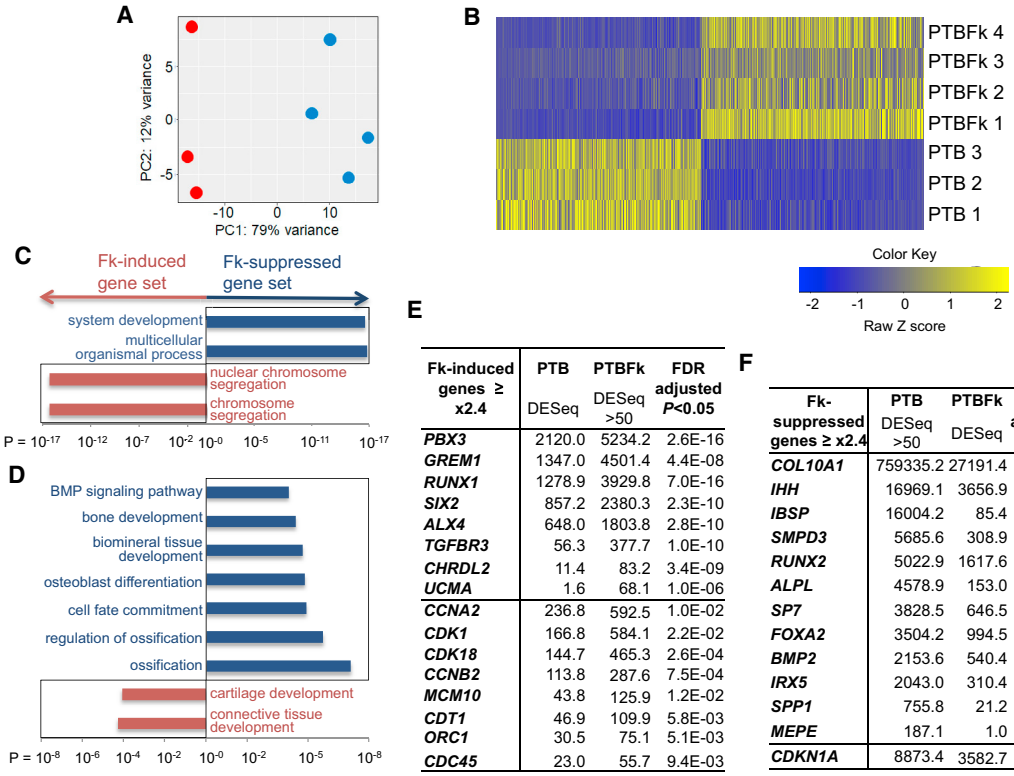

E

Fk-induced genes ≥ x2.4	PTB DESeq	PTBFk DESeq >50	FDR adjusted *P*<0.05
PBX3	2120.0	5234.2	2.6E-16
GREM1	1347.0	4501.4	4.4E-08
RUNX1	1278.9	3929.8	7.0E-16
SIX2	857.2	2380.3	2.3E-10
ALX4	648.0	1803.8	2.8E-10
TGFBR3	56.3	377.7	1.0E-10
CHRDL2	11.4	83.2	3.4E-09
UCMA	1.6	68.1	1.0E-06
CCNA2	236.8	592.5	1.0E-02
CDK1	166.8	584.1	2.2E-02
CDK18	144.7	465.3	2.6E-04
CCNB2	113.8	287.6	7.5E-04
MCM10	43.8	125.9	1.2E-02
CDT1	46.9	109.9	5.8E-03
ORC1	30.5	75.1	5.1E-03
CDC45	23.0	55.7	9.4E-03

F

Fk-suppressed genes ≥ x2.4	PTB DESeq >50	PTBFk DESeq	FDR adjusted *P*<0.05
COL10A1	759335.2	27191.4	1.4E-11
IHH	16969.1	3656.9	1.1E-03
IBSP	16004.2	85.4	4.2E-09
SMPD3	5685.6	308.9	1.2E-06
RUNX2	5022.9	1617.6	2.9E-06
ALPL	4578.9	153.0	5.1E-09
SP7	3828.5	646.5	3.3E-10
FOXA2	3504.2	994.5	1.5E-11
BMP2	2153.6	540.4	6.7E-11
IRX5	2043.0	310.4	1.0E-10
SPP1	755.8	21.2	6.6E-06
MEPE	187.1	1.0	9.2E-16
CDKN1A	8873.4	3582.7	1.5E-16

Figure 5. Comparative Transcriptome Analysis of Cartilage Pellets Using the RNA-seq Technology

(A) Principal component analysis of the expression pattern of protein-coding genes between PTB (PDGF + TGF-β + BMP4, red) and PTBFk (PTB + forskolin, blue) cartilage pellets.

(B) Heatmap of the differentially expressed genes (DEG).

(C and D) Gene ontology (GO) analysis. GO categories for forskolin (Fk)-induced genes (brown bars) and Fk-suppressive genes (blue bars). (C) Top GO categories ($p < 1.0E-17$) from Table S1. (D) Skeletogenesis-related GO terms ($p < 1.0E-04$) from Table S2.

(E and F) Selected lists of Fk-induced genes (E) from Table S3 and Fk-suppressive genes (F) from Table S4.

gene set included the $p21^{CIP1}$ cell-cycle inhibitor gene, *CDKN1A* (Figure 5F, Table S4).

Furthermore, GO analysis suggested that forskolin treatment during chondrogenesis would promote "cartilage development" and "connective tissue development," but suppress "ossification," "osteoblast differentiation," "biomineral tissue development," "bone development," and the "BMP signaling pathway" (Figure 5D, Table S2). In support, the forskolin-induced gene set contained genes associated with chondrogenesis such as *RUNX1* (Yoshida and Komori, 2005), *PBX3* (Capellini et al., 2006), and *TGFBR3*, genes involved in nasal cartilage specification such as *ALX4* (Beverdam et al., 2001) and *SIX2* (He et al., 2010), the mineralization inhibitor gene, *UCMA* (Surmann-Schmitt et al., 2008), and BMP inhibitor genes such as *GREM1* (Leijten et al., 2012) and *CHRDL2* (Nakayama et al., 2004) (Figure 5E, Table S3). In contrast, the forskolin-suppressed gene set included inducers of chondrocyte hypertrophy such as *RUNX2* (de Crombrugghe and Akiyama, 2009), *Osterix/SP7* (Nakashima et al., 2002), and *FOXA2* (Ionescu et al., 2012) as well as *IHH* (Scotti et al., 2010), indicator genes of chondrocyte hypertrophy such as *COL10A1* and *ALPL*, genes associated with (chondrocyte) mineralization and bone formation such as *IBSP*, *SPP1*, *MEPE* (Bonewald et al., 2009), and *IRX5* (Askary et al., 2015), and those associated with BMP and its signaling targets such as *BMP2* and *SMPD3* (Kakoi et al., 2014) (Figure 5F, Table S4). Real-time RT-PCR of some of these genes has confirmed the differential expression (Figure S3B).

These results are strikingly consistent with our previous observations that forskolin treatment keeps the chondrocytes in an immature state by suppressing their commitment to hypertrophic differentiation, probably through enhancement of chondrocyte proliferation (Figures 3C and 3D).

Forskolin-Treated Cartilage Pellets Are Better Maintained in an Unmineralized State *In Vivo* than Untreated Pellets

Based on a prediction from the report of Scotti et al. (2010), we examined whether the suppression by forskolin of the

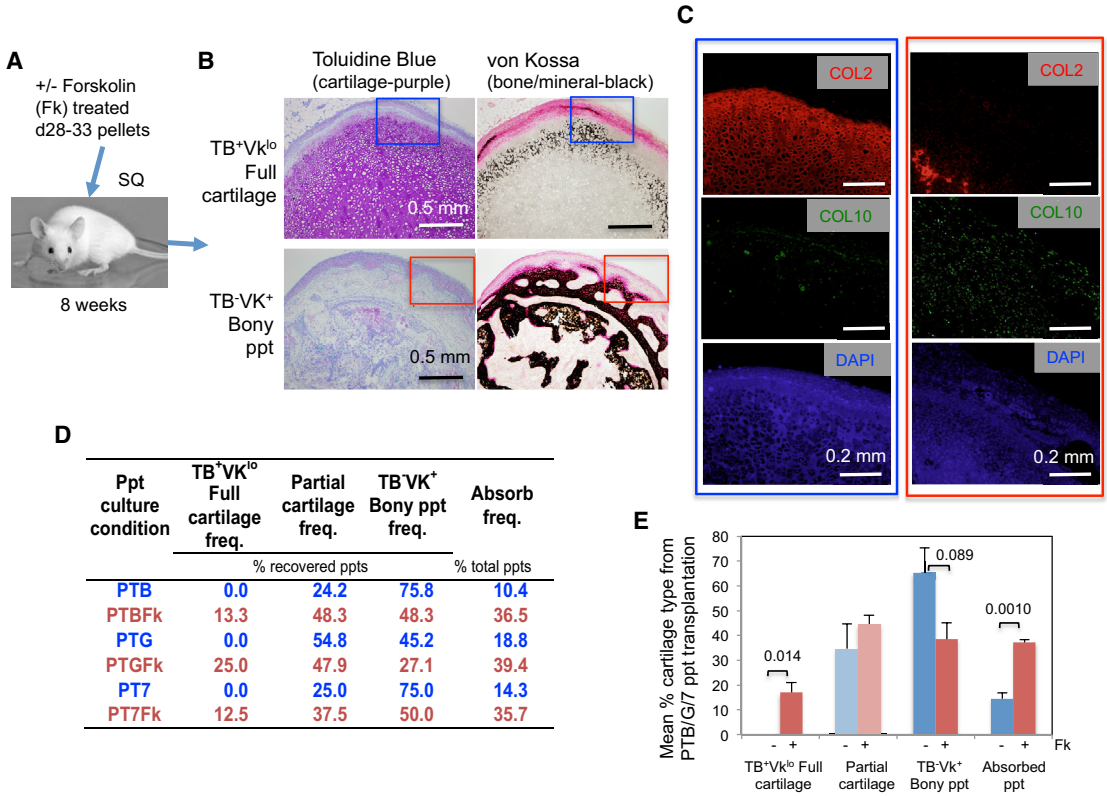

D

Ppt culture condition	TB^+VK^{lo} Full cartilage freq.	Partial cartilage freq.	TB^-VK^+ Bony ppt freq.	Absorb freq.
	% recovered ppts			% total ppts
PTB	0.0	24.2	75.8	10.4
PTBFk	13.3	48.3	48.3	36.5
PTG	0.0	54.8	45.2	18.8
PTGFk	25.0	47.9	27.1	39.4
PT7	0.0	25.0	75.0	14.3
PT7Fk	12.5	37.5	50.0	35.7

Figure 6. *In Vivo* Stability of Cartilage Pellets Formed from hESC-Derived Ectomesenchymal Cells in the Presence of Forskolin

(A and B) Graphical representation of the experimental procedure and examples of recovered cartilage: near-intact toluidine blue $(TB)^+$, von Kossa $(VK)^{lo}$ full cartilage, and completely mineralized TB^-VK^+ bony pellet (ppt). The criteria for the different types of cartilage pellets are summarized in Figures S6A–S6C.

(C) Immunofluorescence study of the TB^+VK^{lo} full cartilage (blue) and the TB^-VK^+ bony ppt (red). See Figure S6D.

(D) Mean frequencies (freq.) of full cartilage, partial cartilage, and bony ppt recovery from transplantation experiments using cartilage pellets (ppts) generated under PTB (PDGF + TGF-β + BMP4), PTB + forskolin (PTBFk), PTG (PDGF + TGF-β + GDF5), PTGFk, PT7 (PDGF + TGF-β + BMP7), or PT7Fk conditions. Mean frequencies of absorption are also shown. Figures S7A and S7B shows graphical representations with statistics.

(E) Mean frequencies of full cartilage, partial cartilage, and bony ppt recovery from all three BMP conditions tested (n = 3) with or without Fk treatment are presented with SEM and p values. Cumulative data and analyses are presented in Figures S7C–S7E.

commitment of chondrocytes to hypertrophic differentiation in cartilage developed *in vitro* would lead to suppression of post-transplantational mineralization of the cartilage. We subjected ectomesenchymal cells to pellet culture for 28–33 days under PTB, PTG, and PT7 conditions with or without forskolin treatment. The resulting pellets were transplanted subcutaneously into NSG mice, harvested 8 weeks later (Figure 6A), and analyzed immunohistochemically. Metachromatic staining of TB, which indicates the presence of sGAG, would confirm the presence of active chondrocytes, whereas black von Kossa staining (VK), a sign of calcium accumulation would indicate chondrocyte mineralization and bone formation. Figures S6A–S6C classify the types of cartilage pellets recovered. Analyses were focused on the TB^+VK^{lo} full-cartilage pellet that maintained cartilaginous matrix (sGAG $[TB^+]$ and COL2) with minimal signs of mineralization (VK^{lo}) and COL10 expression, and the TB^-VK^+ bony pellets that lost sGAG (TB^-) and were fully mineralized (VK^+) but still contained $COL10^+$ hypertrophic chondrocytes (Figures 6B and 6C).

As shown in Figure 6D, the addition of forskolin to PTB-based pellet culture increased the recovery of TB^+VK^{lo} full-cartilage pellets from 0% to 13.3% of total recovered pellets (n [independent transplantation] = 9–10, p = 0.18; not statistically significant; Figure S7A), and led to a concomitant decrease in the frequency of TB^-VK^+ bony pellets from 75.8% to 48.3% (p = 0.050; Figure S7A). Similarly, forskolin addition to PTG culture significantly improved the maintenance *in vivo* of TB^+VK^{lo} cartilage from 0% to 25.0% (n = 7–8, p = 0.023; Figure S7A). Forskolin addition to PT7 culture also improved TB^+VK^{lo} cartilage

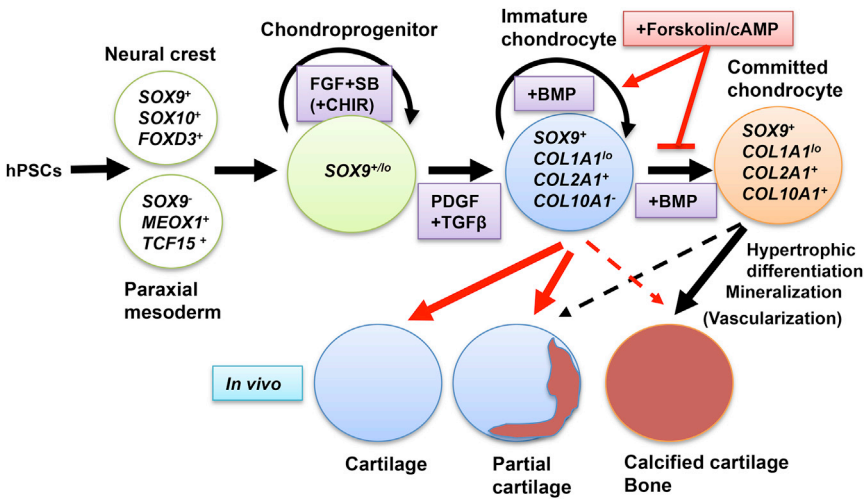

Figure 7. Schematic Representation of the Role of *In Vitro* Forskolin Treatment on the Pre- and Post-transplantational Fate of Cartilage Developed from hPSCs

maintenance from 0% to 12.5% (n = 5–6, p = 0.24, not statistically significant; Figure S7A). Interestingly, however, the recoveries of $TB^{+}VK^{lo}$ full cartilage (increased by forskolin, p = 0.014) and $TB^{-}VK^{+}$ bony pellet (decreased by forskolin, p = 0.089) were surprisingly consistent, regardless of the type of BMP used to promote cartilage pellet formation (Figure 6E). The analysis based on cumulative data led to similar results (Figures S7C–S7E).

In conclusion, while forskolin treatment did not completely inhibit the BMP-promoted commitment of chondrocytes to hypertrophic differentiation during *in vitro* chondrogenesis from ectomesenchymal cells, it significantly and specifically counteracted such effects of BMP (but not BMP-facilitated hyaline chondrogenesis), and improved the maintenance of cartilage at an unmineralized or less mineralized state *in vivo* without loss of the capacity to produce cartilage matrix.

DISCUSSION

We have demonstrated that the commitment of chondrocytes in cartilage pellets developed *in vitro* from the hPSC-derived chondroprogenitors to hypertrophic differentiation can be inhibited by forskolin treatment, and such *in vitro* treatment can have a lasting effect on the fate of the resulting chondrocytes; namely inhibition of further maturation, mineralization, and bone formation, even after transplantation (Figure 7). Furthermore, forskolin achieved this effect, at least in part, by maintaining chondrocytes in a primitive, proliferative state.

We used forskolin as a PTHrP mimic. Attempts to use PTHrP or PTHrP(1–34) peptide to suppress hypertrophic differentiation of chondrocytes developed *in vitro* from MSCs have thus far yielded contradictory results. In earlier studies, PTHrP enhanced COL2 expression and weakly suppresses COL10 expression (Kim et al., 2008). PTHrP in chondrocyte conditioned medium also suppressed COL10 expression (Fischer et al., 2010). However, in later studies, PTHrP was inhibitory for chondrogenesis and suppressed the expression of both *COL2A1* and *COL10A1* (Weiss et al., 2010), although intermittent administration of PTHrP(1–34) was found to alleviate the situation to some extent (Fischer et al., 2014). Chondrogenesis from adult MSCs in the presence of TGF-β induced the expression of *COL2A1* and *COL10A1* simultaneously (Fischer et al., 2014; Weiss et al., 2010). In contrast, chondrogenesis from the hPSC-derived chondroprogenitors showed sequential induction of *COL2A1* then *COL10A1*, so resembling the maturation process of chondrocytes in the growth plate. It is therefore tempting to speculate that our success in the use of forskolin to reproducibly suppress signs of chondrocyte hypertrophic differentiation *in vitro* without affecting hyaline chondrogenesis may be attributed to the stage-specific administration of forskolin (i.e., after *COL2A1* but before *COL10A1* induction) used in our hPSC-derived cell system.

BMPs are known to facilitate the hypertrophic differentiation of chondrocytes *in vitro* at different efficiencies dependent on the BMP used; e.g., GDF5 and BMP7 are not very effective or sometimes inhibitory (Caron et al., 2013; Enochson et al., 2014; Hatakeyama et al., 2004). In fact, BMP7 weakly induced *COL10A1* and *ALPL* expression, and GDF5 induced it to levels between those achieved with BMP7 and BMP4 (Figures 2 and S3A). These differences, however, did not reflect the *in vivo* stability of developed cartilage pellets, so that no cartilage remained as $TB^{+}VK^{lo}$ full cartilage after 8 weeks regardless of BMP (Figures 6D and S7). In addition, conditions without exogenous BMPs (PT condition) have thus far showed no significant

improvements (Figure S7), contrary to the expectation from the previous studies using mesodermal progenitors (Craft et al., 2015). Therefore, the use of no BMP, or a particular type of BMP, could not substitute effectively for forskolin in the promotion of long-lasting cartilage formation from ectomesenchymal cells.

We performed comparative bioinformatics analyses with Wu et al. (2013) human embryonic chondrocyte databases (GEO: GSE51812), but found no significant indications of forskolin-promotion of articular chondrocyte formation in our cultures (Tables S5 and S6), similar to the effects of GREM1, FRZB, and DKK1 on the MSC chondrogenesis (Leijten et al., 2012). However, the GO analysis implicated forskolin suppression of the "BMP signaling pathway" among the most probable biological mechanisms of forskolin (Figure 5D). In fact, we observed that forskolin induced BMP inhibitor gene expression and suppressed BMP signaling gene expression (Figures 2B, 5E, 5F, and S3B, Tables S3 and S4). Since exogenous forskolin and BMPs were not present *in vivo*, suppression of the intrinsic capacity of cartilage pellets to activate BMP signaling may contribute to the improved maintenance of transplanted cartilage pellets at an unmineralized or less mineralized state for 8 weeks.

Significant fractions of the forskolin-treated cartilage pellets recovered from ectopic transplantation were mineralized (Figures 6, S6, and S7), possibly due in part to preferential absorption of unmineralized cartilage pellets generated *in vitro* with forskolin. We have noted that forskolin treatment resulted in increased pellet loss, although only the PTB condition gave statistically significant differences: from 10.4% (PTB) to 36.5% (PTBFk) ($p = 0.084$; Figure S7B). However, the mean increased rate of loss of forskolin-treated pellets was consistent, regardless of the type of BMP used for cartilage pellet formation ($p = 0.0010$; Figure 6E). Furthermore, the results may be due to the background expression of hypertrophy-inducer genes such as *RUNX2*, *SP7*, *BMP2*, and *BMP4*, which was not completely suppressed by forskolin. These gene products may be upregulated and become functional after transplantation to promote mineralized cartilage formation. Additional blocking of WNT signaling by a porcupine inhibitor did not significantly improve the *in vitro* effect (Figure 3B) and *in vivo* consequence (data not shown) of forskolin treatment. Therefore, manipulation of other mechanisms may be needed.

Thus, one of the advantages of the hPSC-derived chondroprogenitor cell system for generating tissue-engineered cartilage is that the post-transplantational fate of developed chondrocytes can be more robustly controlled at a pre-transplantational stage (i.e., *in vitro*), compared with the adult MSC systems reported (Fischer et al., 2010; Narcisi et al., 2015; Weiss et al., 2010). Mechanistic studies to understand how these processes work are necessary, not only to improve the efficacy of hPSC-based cartilage regenerative therapy but also to apply the mechanism to the more clinically relevant adult stem cells for better therapeutic outcomes.

EXPERIMENTAL PROCEDURES

Human Pluripotent Stem Cell Culture

H9 (WA09) hESCs from WiCell were maintained on mouse embryonic fibroblast feeder cells. CY2-SOX9-2A-ZsGreen-2A-Puro (SOX9-GFP) hiPSCs from NIH were maintained in E8 medium as described (Umeda et al., 2015). Human PSC experiments were under the regulation of SCRO for the University of Texas Health Science Center at Houston (UTHealth).

Generation and Expansion of Ectomesenchymal Cells from hPSCs through Neural Crest Specification

Human ESCs and iPSCs were differentiated, and the neural crest-like progeny were purified by fluorescence-activated cell sorting (FACS) and expanded as described (Umeda et al., 2015).

Generation and Expansion of Paraxial Mesoderm from hPSCs

Human ESCs were differentiated using the improved embryoid-body-forming culture method (Umeda et al., 2015). Paraxial mesoderm cells were isolated by FACS as described (Umeda et al., 2012), and were then expanded in CDM (Umeda et al., 2015) supplemented with FGF2, PDGF, SB431542, and CHIR99021 (FPSbC medium). At passage 2, PDGF was removed (FSbC).

Expansion of Human Adult Nasal Chondrocytes

Human adult nasal chondrocytes from one female (11F) and two male patients (12M, 13M) were independently isolated and expanded to passage 3 as described (Centola et al., 2013).

Scaffold-free Cartilage Formation: Pellet Culture

Chondrogenesis was induced by pellet culture as described (Umeda et al., 2015). Chondrogenesis from human nasal chondrocytes was performed as described (Pelttari et al., 2014).

Isolation of Chondrocytes from Cartilage Pellets

A cartilage pellet was treated with 4 mg/mL collagenase in the pellet culture medium (Umeda et al., 2015) at 37°C for 3 hr and dissociated to single cells by repetitive pipetting.

Isolation and Quantification of DNA, RNA, and sGAG from Cartilage

DNAs and sGAGs from cartilage pellets were isolated, quantified, and analyzed as described (Umeda et al., 2015).

EdU Incorporation Assay

Cartilage pellets were labeled with EdU for 21–25 hr. Then chondrocytes were isolated and processed using the Click-iT plus EdU Alexa Fluor 647 Kit (Invitrogen) and analyzed by FACS.

Gene Expression Profiling

Real-time RT-PCR experiments were performed as described (Umeda et al., 2015). The results are presented as mean relative expression levels (against *EEF1A1*) with SEM shown by thin error lines. The change in expression was a relative expression of a gene in treated (+) pellets normalized against that in the corresponding untreated (−) pellets. RNA sequencing (RNA-seq) was performed on an Illumina Nextseq500. Sequenced reads (GEO: GSE116173) were mapped against the human reference genome (hg19). Expression levels were calculated as normalized gene counts from DESeq2 (Figure 5, Tables S1–S4).

Subcutaneous Transplantation of Cartilage Particles

The subcutaneous transplantation was performed as described (Umeda et al., 2015), under the regulation of IACUC for UTHealth.

Immunohistological Staining

The cartilage pellets made *in vitro* were fixed with Zn-formalin, paraffin embedded, sectioned, and subjected to immunofluorescence detection of COL1, COL2, and Ki67.

Statistical Analysis

Statistical differences between groups were determined by Student's t test (2 categories) or one-way ANOVA(>2 categories) followed by the Student-Newman-Keuls multiple comparisons. n is the number of independent experiments. $p < 0.2$ values are shown as numbers in the bar graphs. Mean values that give $p \geq 0.1$ from the +/− treatment comparisons are shown in light-colored bars.

Note Added in Proof

During revision of this manuscript, Wu et al. (2017) published a report demonstrating that inhibition of κ-opioid receptor/cAMP signaling accelerated the degeneration of injured articular cartilage.

SUPPLEMENTAL INFORMATION

Supplemental Information includes Supplemental Experimental Procedures, seven figures, and seven tables and can be found with this article online at https://doi.org/10.1016/j.stemcr.2018.06.021.

AUTHOR CONTRIBUTIONS

J.Y.L. performed the initial hPSC-derived ectomesenchymal cell experiments and RT-PCR analyses, analyzed data, and wrote the first draft of the manuscript; N.M. performed immunofluorescence staining and transplantation experiments; A.P. performed cartilage pellet formation and RT-PCR; B.K.A. performed additional ectomesenchymal cell experiments; M.L. made the RNA-seq libraries and performed sequencing; and J.L. and D.S. performed bioinformatics analyses. Y.H. oversaw the RNA-seq and bioinformatics analyses; S.P. and I.M. isolated and expanded human adult nasal chondrocytes; J.H. provided knowledge through regular discussion of experiments and revised the manuscript; and N.N. designed and directed the research, performed additional experiments, analyzed data, and completed the manuscript. N.M. and A.P. contributed equally.

ACKNOWLEDGMENTS

We would like to acknowledge A. Hazen and A. Blancas for cell sorting, A. Blancas, Z. Mao, S. Amra, and M. Starbuck for histological analyses, and Z. Mao for immunofluorescence analyses. This work was supported by the Brown Foundation Institute of Molecular Medicine start-up fund (N.N.), the Annie and Bob Graham Distinguished Chair in Stem Cell Biology (N.N.), Cancer Prevention and Research Institute of Texas (RR140053, Y.H.), the John S. Dunn Foundation Collaborative Research Award (Y.H.), the NIH (R01HL134780, Y.H.), and an allocation from the Texas A&M University start-up funds (Y.H. and D.S.).

Received: June 26, 2017
Revised: June 28, 2018
Accepted: June 29, 2018
Published: July 26, 2018

REFERENCES

Amizuka, N., Warshawsky, H., Henderson, J.E., Goltzman, D., and Karaplis, A.C. (1994). Parathyroid hormone-related peptide-depleted mice show abnormal epiphyseal cartilage development and altered endochondral bone formation. J. Cell Biol. *126*, 1611–1623.

Askary, A., Mork, L., Paul, S., He, X., Izuhara, A.K., Gopalakrishnan, S., Ichida, J.K., McMahon, A.P., Dabizljevic, S., Dale, R., et al. (2015). Iroquois proteins promote skeletal joint formation by maintaining chondrocytes in an immature state. Dev. Cell *35*, 358–365.

Beverdam, A., Brouwer, A., Reijnen, M., Korving, J., and Meijlink, F. (2001). Severe nasal clefting and abnormal embryonic apoptosis in Alx3/Alx4 double mutant mice. Development *128*, 3975–3986.

Bonewald, L.F., Dallas, S.L., and Gorski, J.P. (2009). Bone mineralization. In The Skeletal System, O. Pourquié, ed. (Cold Spring Harbor Laboratory Press), pp. 277–295.

Breckler, M., Berthouze, M., Laurent, A.C., Crozatier, B., Morel, E., and Lezoualc'h, F. (2011). Rap-linked cAMP signaling Epac proteins: compartmentation, functioning and disease implications. Cell Signal. *23*, 1257–1266.

Buckwalter, J.A., Marsh, J.L., Brown, T., Amendola, A., and Martin, J.A. (2014). Articular cartilage injury. In Principles of Tissue Engineering, R. Lanza, R. Langer, and J.P. Vacanti, eds. (Academic Press), pp. 1253–1266.

Capellini, T.D., Di Giacomo, G., Salsi, V., Brendolan, A., Ferretti, E., Srivastava, D., Zappavigna, V., and Selleri, L. (2006). Pbx1/Pbx2 requirement for distal limb patterning is mediated by the hierarchical control of Hox gene spatial distribution and Shh expression. Development *133*, 2263–2273.

Caron, M.M., Emans, P.J., Cremers, A., Surtel, D.A., Coolsen, M.M., van Rhijn, L.W., and Welting, T.J. (2013). Hypertrophic differentiation during chondrogenic differentiation of progenitor cells is stimulated by BMP-2 but suppressed by BMP-7. Osteoarthritis Cartilage *21*, 604–613.

Centola, M., Abbruzzese, F., Scotti, C., Barbero, A., Vadala, G., Denaro, V., Martin, I., Trombetta, M., Rainer, A., and Marsano, A. (2013). Scaffold-based delivery of a clinically relevant anti-angiogenic drug promotes the formation of in vivo stable cartilage. Tissue Eng. Part A *19*, 1960–1971.

Chen, X., Macica, C.M., Nasiri, A., and Broadus, A.E. (2008). Regulation of articular chondrocyte proliferation and differentiation by Indian hedgehog and parathyroid hormone-related protein in mice. Arthritis Rheum. *58*, 3788–3797.

Christensen, A.E., Selheim, F., de Rooij, J., Dremier, S., Schwede, F., Dao, K.K., Martinez, A., Maenhaut, C., Bos, J.L., Genieser, H.G., et al. (2003). cAMP analog mapping of Epac1 and cAMP kinase. Discriminating analogs demonstrate that Epac and cAMP kinase act synergistically to promote PC-12 cell neurite extension. J. Biol. Chem. *278*, 35394–35402.

Craft, A.M., Rockel, J.S., Nartiss, Y., Kandel, R.A., Alman, B.A., and Keller, G.M. (2015). Generation of articular chondrocytes from human pluripotent stem cells. Nat. Biotechnol. *33*, 638–645.

de Crombrugghe, B., and Akiyama, H. (2009). Transcriptional control of chondrocyte differentiation. In The Skeletal System, O. Pourquié, ed. (Cold Spring Harbor Laboratory Press), pp. 147–170.

Enochson, L., Stenberg, J., Brittberg, M., and Lindahl, A. (2014). GDF5 reduces MMP13 expression in human chondrocytes via DKK1 mediated canonical Wnt signaling inhibition. Osteoarthritis Cartilage *22*, 566–577.

Fischer, J., Dickhut, A., Rickert, M., and Richter, W. (2010). Human articular chondrocytes secrete parathyroid hormone-related protein and inhibit hypertrophy of mesenchymal stem cells in coculture during chondrogenesis. Arthritis Rheum. *62*, 2696–2706.

Fischer, J., Aulmann, A., Dexheimer, V., Grossner, T., and Richter, W. (2014). Intermittent PTHrP(1-34) exposure augments chondrogenesis and reduces hypertrophy of mesenchymal stromal cells. Stem Cells Dev. *23*, 2513–2523.

Guo, J., Chung, U.I., Yang, D., Karsenty, G., Bringhurst, F.R., and Kronenberg, H.M. (2006). PTH/PTHrP receptor delays chondrocyte hypertrophy via both Runx2-dependent and -independent pathways. Dev. Biol. *292*, 116–128.

Hatakeyama, Y., Tuan, R.S., and Shum, L. (2004). Distinct functions of BMP4 and GDF5 in the regulation of chondrogenesis. J. Cell. Biochem. *91*, 1204–1217.

He, G., Tavella, S., Hanley, K.P., Self, M., Oliver, G., Grifone, R., Hanley, N., Ward, C., and Bobola, N. (2010). Inactivation of Six2 in mouse identifies a novel genetic mechanism controlling development and growth of the cranial base. Dev. Biol. *344*, 720–730.

Huang, W., Zhou, X., Lefebvre, V., and de Crombrugghe, B. (2000). Phosphorylation of SOX9 by cyclic AMP-dependent protein kinase A enhances SOX9's ability to transactivate a Col2a1 chondrocyte-specific enhancer. Mol. Cell. Biol. *20*, 4149–4158.

Huang, W., Chung, U.I., Kronenberg, H.M., and de Crombrugghe, B. (2001). The chondrogenic transcription factor Sox9 is a target of signaling by the parathyroid hormone-related peptide in the growth plate of endochondral bones. Proc. Natl. Acad. Sci. USA *98*, 160–165.

Ionescu, A., Kozhemyakina, E., Nicolae, C., Kaestner, K.H., Olsen, B.R., and Lassar, A.B. (2012). FoxA family members are crucial regulators of the hypertrophic chondrocyte differentiation program. Dev. Cell *22*, 927–939.

Kakoi, H., Maeda, S., Shinohara, N., Matsuyama, K., Imamura, K., Kawamura, I., Nagano, S., Setoguchi, T., Yokouchi, M., Ishidou, Y., et al. (2014). Bone morphogenic protein (BMP) signaling upregulates neutral sphingomyelinase 2 to suppress chondrocyte maturation via the Akt protein signaling pathway as a negative feedback mechanism. J. Biol. Chem. *289*, 8135–8150.

Karaplis, A.C., Luz, A., Glowacki, J., Bronson, R.T., Tybulewicz, V.L., Kronenberg, H.M., and Mulligan, R.C. (1994). Lethal skeletal dysplasia from targeted disruption of the parathyroid hormone-related peptide gene. Genes Dev. *8*, 277–289.

Kim, Y.J., Kim, H.J., and Im, G.I. (2008). PTHrP promotes chondrogenesis and suppresses hypertrophy from both bone marrow-derived and adipose tissue-derived MSCs. Biochem. Biophys. Res. Commun. *373*, 104–108.

Kozhemyakina, E., Cohen, T., Yao, T.P., and Lassar, A.B. (2009). Parathyroid hormone-related peptide represses chondrocyte hypertrophy through a protein phosphatase 2A/histone deacetylase 4/MEF2 pathway. Mol. Cell. Biol. *29*, 5751–5762.

Lanske, B., Karaplis, A.C., Lee, K., Luz, A., Vortkamp, A., Pirro, A., Karperien, M., Defize, L.H., Ho, C., Mulligan, R.C., et al. (1996). PTH/PTHrP receptor in early development and Indian hedgehog-regulated bone growth. Science *273*, 663–666.

Leijten, J.C., Emons, J., Sticht, C., van Gool, S., Decker, E., Uitterlinden, A., Rappold, G., Hofman, A., Rivadeneira, F., Scherjon, S., et al. (2012). Gremlin 1, frizzled-related protein, and Dkk-1 are key regulators of human articular cartilage homeostasis. Arthritis Rheum. *64*, 3302–3312.

Li, T.F., Dong, Y., Ionescu, A.M., Rosier, R.N., Zuscik, M.J., Schwarz, E.M., O'Keefe, R.J., and Drissi, H. (2004). Parathyroid hormone-related peptide (PTHrP) inhibits Runx2 expression through the PKA signaling pathway. Exp. Cell Res. *299*, 128–136.

Malemud, C.J., Mills, T.M., Shuckett, R., and Papay, R.S. (1986). Stimulation of sulfated-proteoglycan synthesis by forskolin in monolayer cultures of rabbit articular chondrocytes. J. Cell. Physiol. *129*, 51–59.

Minina, E., Kreschel, C., Naski, M.C., Ornitz, D.M., and Vortkamp, A. (2002). Interaction of FGF, Ihh/Pthlh, and BMP signaling integrates chondrocyte proliferation and hypertrophic differentiation. Dev. Cell *3*, 439–449.

Nakashima, K., Zhou, X., Kunkel, G., Zhang, Z., Deng, J.M., Behringer, R.R., and de Crombrugghe, B. (2002). The novel zinc finger-containing transcription factor osterix is required for osteoblast differentiation and bone formation. Cell *108*, 17–29.

Nakayama, N., and Umeda, K. (2011). From pluripotent stem cells to lineage-specific chondrocytes: essential signalling and cellular intermediates. In Embryonic Stem Cells: The Hormonal Regulation of Pluripotency and Embryogenesis, C. Atwood, ed. (INTECH), pp. 621–648.

Nakayama, N., Han, C.Y., Cam, L., Lee, J.I., Pretorius, J., Fisher, S., Rosenfeld, R., Scully, S., Nishinakamura, R., Duryea, D., et al. (2004). A novel chordin-like BMP inhibitor, CHL2, expressed preferentially in chondrocytes of developing cartilage and osteoarthritic joint cartilage. Development *131*, 229–240.

Nakayama, N., Lee, J.Y., Matthias, N., Umeda, K., Yan, Q., and Huard, J. (2016). Cartilage regeneration using pluripotent stem cell-derived chondroprogenitors: promise and challenges. In Pluripotent Stem Cells, M. Tomizawa, ed. (INTECH), pp. 385–425.

Namba, R.S., Meuli, M., Sullivan, K.M., Le, A.X., and Adzick, N.S. (1998). Spontaneous repair of superficial defects in articular cartilage in a fetal lamb model. J. Bone Joint Surg. Am. *80*, 4–10.

Narcisi, R., Cleary, M.A., Brama, P.A., Hoogduijn, M.J., Tuysuz, N., ten Berge, D., and van Osch, G.J. (2015). Long-term expansion, enhanced chondrogenic potential, and suppression of endochondral ossification of adult human MSCs via WNT signaling modulation. Stem Cell Reports *4*, 459–472.

Otto, T., and Sicinski, P. (2017). Cell cycle proteins as promising targets in cancer therapy. Nat. Rev. Cancer *17*, 93–115.

Pelttari, K., Pippenger, B., Mumme, M., Feliciano, S., Scotti, C., Mainil-Varlet, P., Procino, A., von Rechenberg, B., Schwamborn, T., Jakob, M., et al. (2014). Adult human neural crest-derived cells for articular cartilage repair. Sci. Transl. Med. *6*, 251ra119.

Pitsillides, A.A., and Beier, F. (2011). Cartilage biology in osteoarthritis–lessons from developmental biology. Nat. Rev. Rheumatol. *7*, 654–663.

Poppe, H., Rybalkin, S.D., Rehmann, H., Hinds, T.R., Tang, X.B., Christensen, A.E., Schwede, F., Genieser, H.G., Bos, J.L., Doskeland, S.O., et al. (2008). Cyclic nucleotide analogs as probes of signaling pathways. Nat. Methods *5*, 277–278.

Sakamoto, A., Chen, M., Kobayashi, T., Kronenberg, H.M., and Weinstein, L.S. (2005). Chondrocyte-specific knockout of the G protein G(s)alpha leads to epiphyseal and growth plate abnormalities and ectopic chondrocyte formation. J. Bone Miner. Res. *20*, 663–671.

Sclafani, R.A., and Holzen, T.M. (2007). Cell cycle regulation of DNA replication. Annu. Rev. Genet. *41*, 237–280.

Scotti, C., Tonnarelli, B., Papadimitropoulos, A., Scherberich, A., Schaeren, S., Schauerte, A., Lopez-Rios, J., Zeller, R., Barbero, A., and Martin, I. (2010). Recapitulation of endochondral bone formation using human adult mesenchymal stem cells as a paradigm for developmental engineering. Proc. Natl. Acad. Sci. USA *107*, 7251–7256.

Somoza, R.A., Welter, J.F., Correa, D., and Caplan, A.I. (2014). Chondrogenic differentiation of mesenchymal stem cells: challenges and unfulfilled expectations. Tissue Eng. Part B Rev. *20*, 596–608.

Steinert, A.F., Ghivizzani, S.C., Rethwilm, A., Tuan, R.S., Evans, C.H., and Noth, U. (2007). Major biological obstacles for persistent cell-based regeneration of articular cartilage. Arthritis Res. Ther. *9*, 213.

Surmann-Schmitt, C., Dietz, U., Kireva, T., Adam, N., Park, J., Tagariello, A., Onnerfjord, P., Heinegard, D., Schlotzer-Schrehardt, U., Deutzmann, R., et al. (2008). Ucma, a novel secreted cartilage-specific protein with implications in osteogenesis. J. Biol. Chem. *283*, 7082–7093.

Tsumaki, N., Nakase, T., Miyaji, T., Kakiuchi, M., Kimura, T., Ochi, T., and Yoshikawa, H. (2002). Bone morphogenetic protein signals are required for cartilage formation and differently regulate joint development during skeletogenesis. J. Bone Miner. Res. *17*, 898–906.

Umeda, K., Zhao, J., Simmons, P., Stanley, E., Elefanty, A., and Nakayama, N. (2012). Human chondrogenic paraxial mesoderm, directed specification and prospective isolation from pluripotent stem cells. Sci. Rep. *2*, 455.

Umeda, K., Oda, H., Yan, Q., Matthias, N., Zhao, J., Davis, B.R., and Nakayama, N. (2015). Long-term expandable SOX9(+) chondrogenic ectomesenchymal cells from human pluripotent stem cells. Stem Cell Reports *4*, 712–726.

van der Kraan, P.M., and van den Berg, W.B. (2012). Chondrocyte hypertrophy and osteoarthritis: role in initiation and progression of cartilage degeneration? Osteoarthritis Cartilage *20*, 223–232.

Vortkamp, A., Lee, K., Lanske, B., Segre, G.V., Kronenberg, H.M., and Tabin, C.J. (1996). Regulation of rate of cartilage differentiation by Indian hedgehog and PTH-related protein. Science *273*, 613–622.

Weiss, S., Hennig, T., Bock, R., Steck, E., and Richter, W. (2010). Impact of growth factors and PTHrP on early and late chondrogenic differentiation of human mesenchymal stem cells. J. Cell. Physiol. *223*, 84–93.

Wu, L., Bluguermann, C., Kyupelyan, L., Latour, B., Gonzalez, S., Shah, S., Galic, Z., Ge, S., Zhu, Y., Petrigliano, F.A., et al. (2013). Human developmental chondrogenesis as a basis for engineering chondrocytes from pluripotent stem cells. Stem Cell Reports *1*, 575–589.

Wu, L., Zhang, S., Shkhyan, R., Lee, S., Gullo, F., Eliasberg, C.D., Petrigliano, F.A., Ba, K., Wang, J., Lin, Y., et al. (2017). Kappa opioid receptor signaling protects cartilage tissue against posttraumatic degeneration. JCI Insight *2*, e88553.

Yamashita, A., Morioka, M., Yahara, Y., Okada, M., Kobayashi, T., Kuriyama, S., Matsuda, S., and Tsumaki, N. (2015). Generation of scaffoldless hyaline cartilaginous tissue from human iPSCs. Stem Cell Reports *4*, 404–418.

Yoshida, C.A., and Komori, T. (2005). Role of Runx proteins in chondrogenesis. Crit. Rev. Eukaryot. Gene Expr. *15*, 243–254.

Zhang, M., Xie, R., Hou, W., Wang, B., Shen, R., Wang, X., Wang, Q., Zhu, T., Jonason, J.H., and Chen, D. (2009). PTHrP prevents chondrocyte premature hypertrophy by inducing cyclin-D1-dependent Runx2 and Runx3 phosphorylation, ubiquitylation and proteasomal degradation. J. Cell Sci. *122*, 1382–1389.

Stem Cell Reports, Volume *11*

Supplemental Information

Pre-transplantational Control of the Post-transplantational Fate of Human Pluripotent Stem Cell-Derived Cartilage

John Y. Lee, Nadine Matthias, Azim Pothiawala, Bryan K. Ang, Minjung Lee, Jia Li, Deqiang Sun, Sebastien Pigeot, Ivan Martin, Johnny Huard, Yun Huang, and Naoki Nakayama

1. SUPPLEMENTAL FIGURES

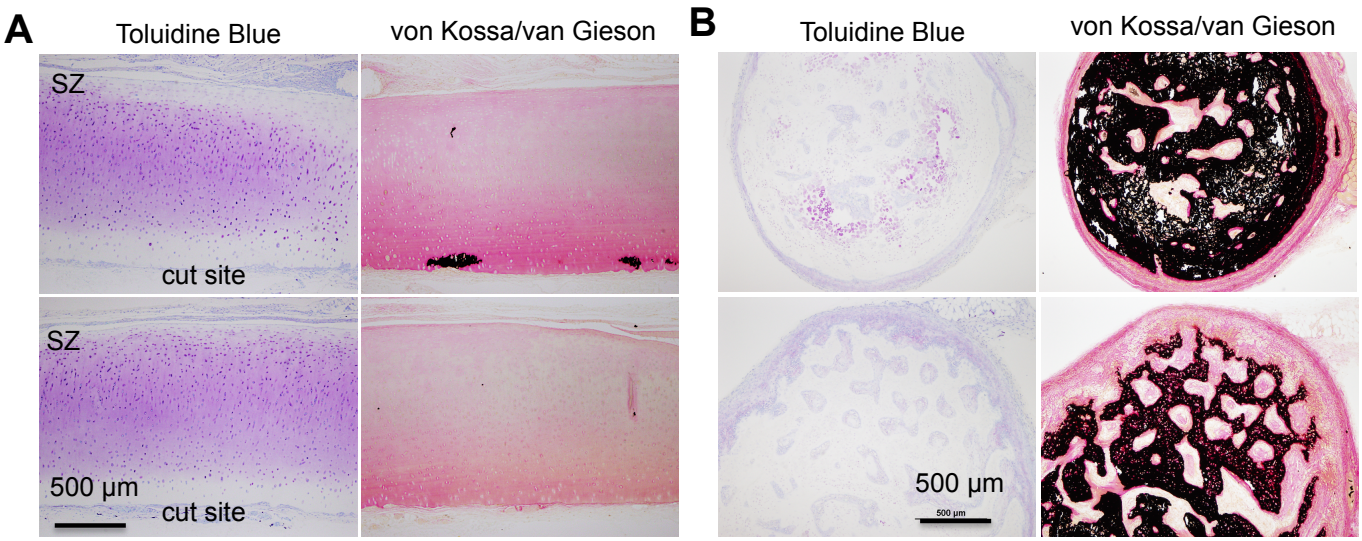

Fig. S1 *In vivo* cartilage stability assayed by subcutaneous transplantation into NSG mice. **(A) Bovine articular cartilage.** A piece of 2-year-old bovine knee articular cartilage subcutaneously transplanted for 12 weeks in NSG mice. Note that some areas of the cut site (in mid zone) but not the untouched natural surface (superficial zone, SZ) were mineralized. **(B) Cartilage pellet from FSbC-expanded human paraxial mesoderm.** Bony tissue with no cartilaginous areas (Toluidine Blue $[TB]^-$ von Kossa $[VK]^+$) detected 9 weeks after subcutaneous transplantation of cartilage pellets developed under PTB (PDGF+TGFβ+BMP4) conditions from expanded hESC-derived paraxial mesodermal cells (passage 4). They were more prone to mineralization than cartilage pellets made with uncultured paraxial mesoderm (Umeda, et al. 2015). Supplementary to Fig. 6.

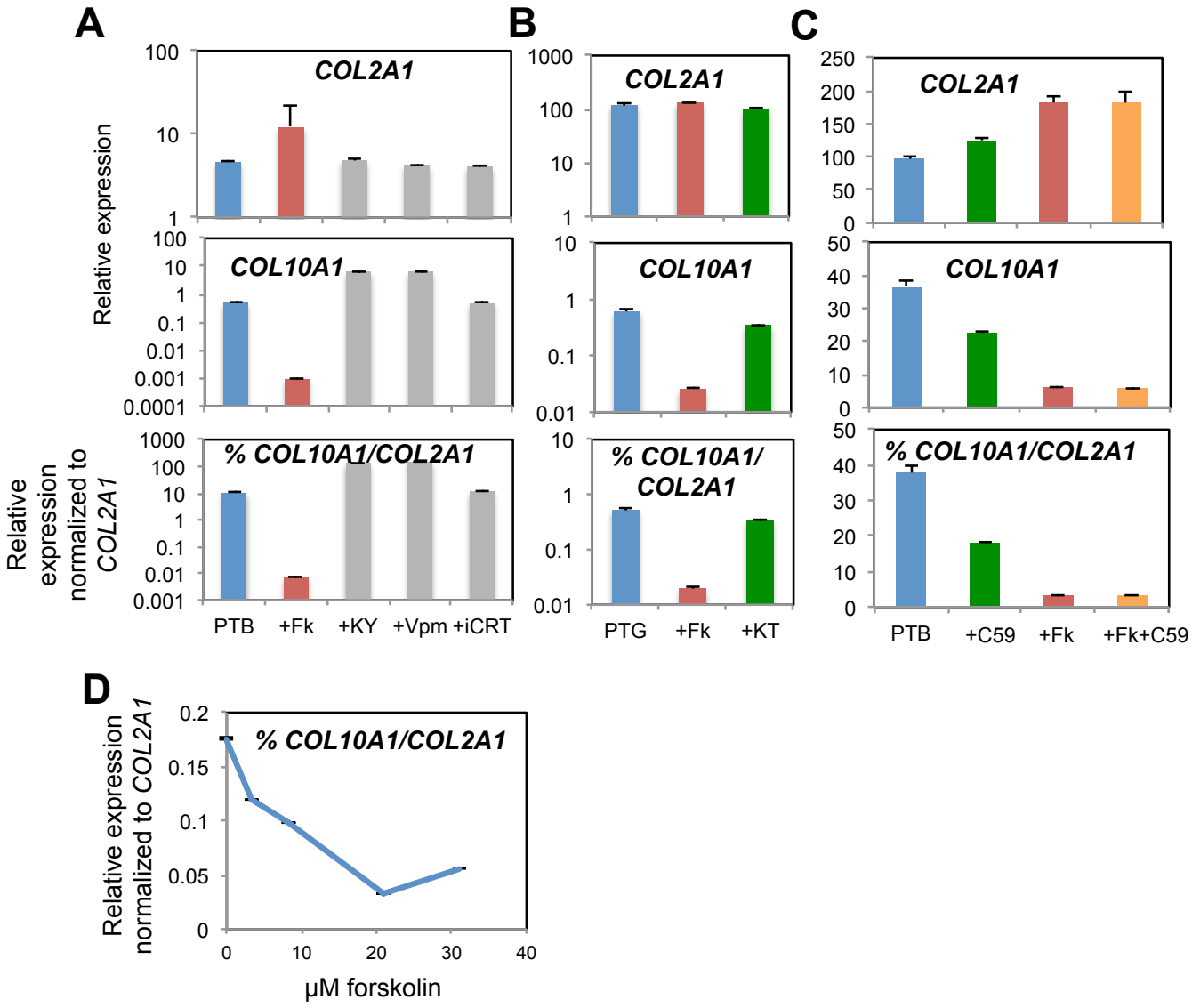

Fig. S2 Functional screening by RT-PCR of small molecules that suppress hypertrophic differentiation of chondrocytes.

(**A-C**) Chondrogenesis using hESC-derived ectomesenchymal cells was performed under PTB (PDGF+TGFβ+BMP4) or PTG (PDGF+TGFβ+GDF5) conditions with forskolin (Fk), KY02111 (KY), Verapamil (Vpm) or iCRT14 (iCRT) (**A**), with Fk or KT5823 (KT) (**B**), and with Fk, 30 nM Wnt-C59 (C59), or Fk+C59 (**C**). The small molecules were added on day 11, except for C59, which was added on day 24. Pellets were harvested on day 32. (**D**) Chondrogenesis using hESC-derived ectomesenchymal cells was performed with 3, 9, 20, and 30 μM forskolin. Supplementary to Fig. 1D-G.

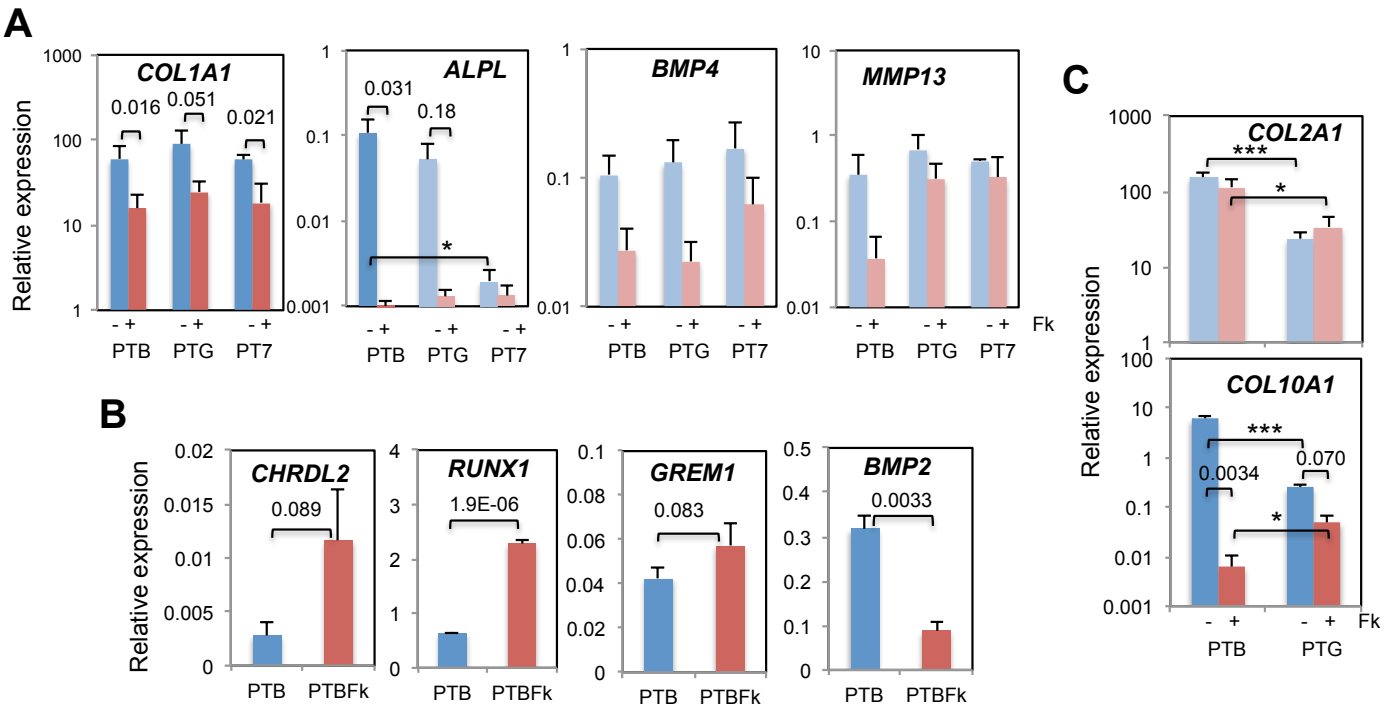

Fig. S3 Gene expression profiling by RT-PCR in forskolin-treated and untreated cartilage pellets. (**A, B**) Chondrogenesis using hESC-derived ectomesenchymal cells was performed under PTB (PDGF+TGFβ+BMP4), PTG (PDGF+TGFβ+GDF5), and PT7 (PDGF+TGFβ+BMP7) conditions, with (Brown: +Fk) or without (Blue: -Fk) forskolin. (**A**) Mean expression levels of chondrocyte genes are shown with SEM and *P*-values (+/-Fk comparison, values of *P*>0.2 are not shown). *COL1A1*: n (independent experiments)=7, *ALPL*: n=3-5, other comparisons **P*=0.10, *BMP4*: n=3, *MMP13*: n=3. Supplementary to Fig. 2A. (**B**) RT-PCR confirmation of RNA-seq data. n=3-4. Supplementary to Fig. 5EF. (**C**) Cartilage from SOX9-GFP hiPSC-derived ectomesenchymal cells made under PTB and PTG conditions with (brown) or without (blue) Fk. Mean expression levels with SEM and *P*-values (+/-Fk comparison) are shown (n=3-4). Supplementary to Fig. 1G. Other comparisons: *COL2A1*: **P*=0.070, ***P*=0.0035, *COL10A1*: **P*=0.083, ***P*=0.0034.

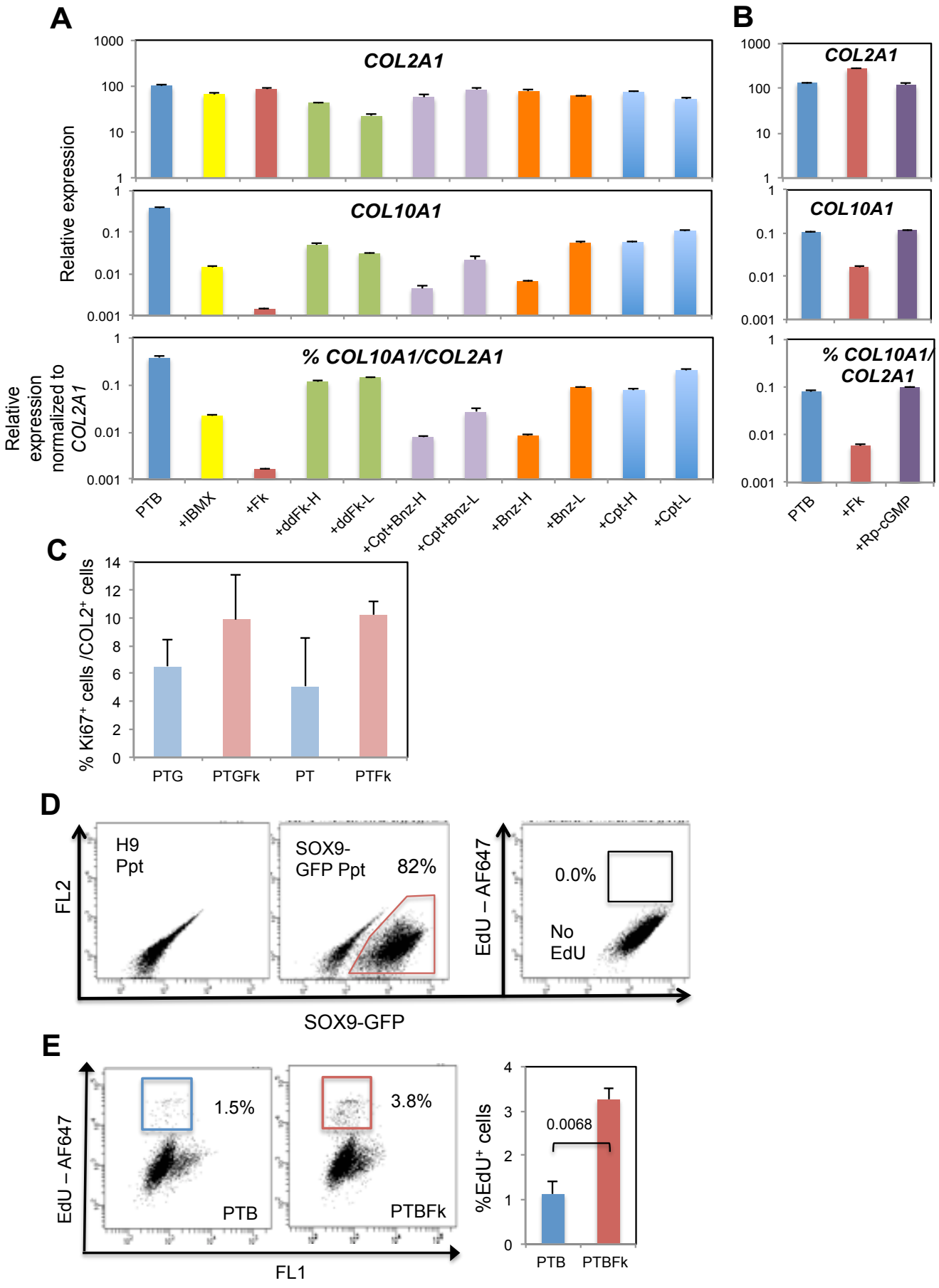
A
COL2A1
COL10A1
% COL10A1/COL2A1
Relative expression
Relative expression normalized to COL2A1
1000
100
10
1
0.1
0.01
0.001
PTB
+IBMX
+Fk
+ddFk-H
+ddFk-L
+Cpt+Bnz-H
+Cpt+Bnz-L
+Bnz-H
+Bnz-L
+Cpt-H
+Cpt-L
B
COL2A1
COL10A1
% COL10A1/ COL2A1
PTB
+Fk
+Rp-cGMP
C
% Ki67+ cells /COL2+ cells
14
12
10
8
6
4
2
0
PTG
PTGFk
PT
PTFk
D
H9 Ppt
SOX9-GFP Ppt
82%
0.0%
No EdU
FL2
EdU – AF647
SOX9-GFP
E
1.5%
3.8%
PTB
PTBFk
EdU – AF647
FL1
%EdU+ cells
0.0068
4
3
2
1
0
PTB
PTBFk

Fig. S4 Effect of cAMP/cGMP analogs on *COL10A1* expression during chondrogenesis.
Chondrogenesis using hESC-derived ectomesenchymal cells was performed under PTB (PDGF+TGFβ+BMP4) conditions for 33 days (**A**) with 0.5 mM IBMX, 25 μM forskolin (Fk), 12.5 μM (L) and 25 μM (H) 1,9-dideoxyforskolin (ddFk), 3 μM (L) and 6 μM (H) CPT-cAMP (Cpt), 40 μM (L) and 80 μM (H) Bnz-cAMP (Bnz), 3 μM CPT-cAMP+40 μM Bnz-cAMP (Cpt+Bnz-L), and 6 μM CPT-cAMP+80 μM Bnz-cAMP (Cpt+Bnz-H), and (**B**) with 25 μM forskolin (Fk), and 60 μM Rp-cGMP, added on day 11. Supplementary to Fig. 3A.

Forskolin effects on the proliferation of chondrocytes in cartilage pellets.
(**C**) Ki67 staining. PTG (PDGF+TGFβ+GDF5) vs. PTG+forskolin (PTGFk): *P*=0.40 (n=4). PT (PDGF+TGFβ) vs. PTFk: *P*=0.28 (n=2-3). Statistically insignificant differences. Supplementary to Fig. 3C (**D**) Without EdU labeling control for Fig. 3D. (**E**) EdU labeling of Fk treated and untreated cartilage pellets generated from H9 hESC-derived ectomesenchymal cells. Left Panels: representative FACS plots. Right panel: Mean % positive cells with SEM and *P*-value. n=3. Supplementary to Fig. 3D.

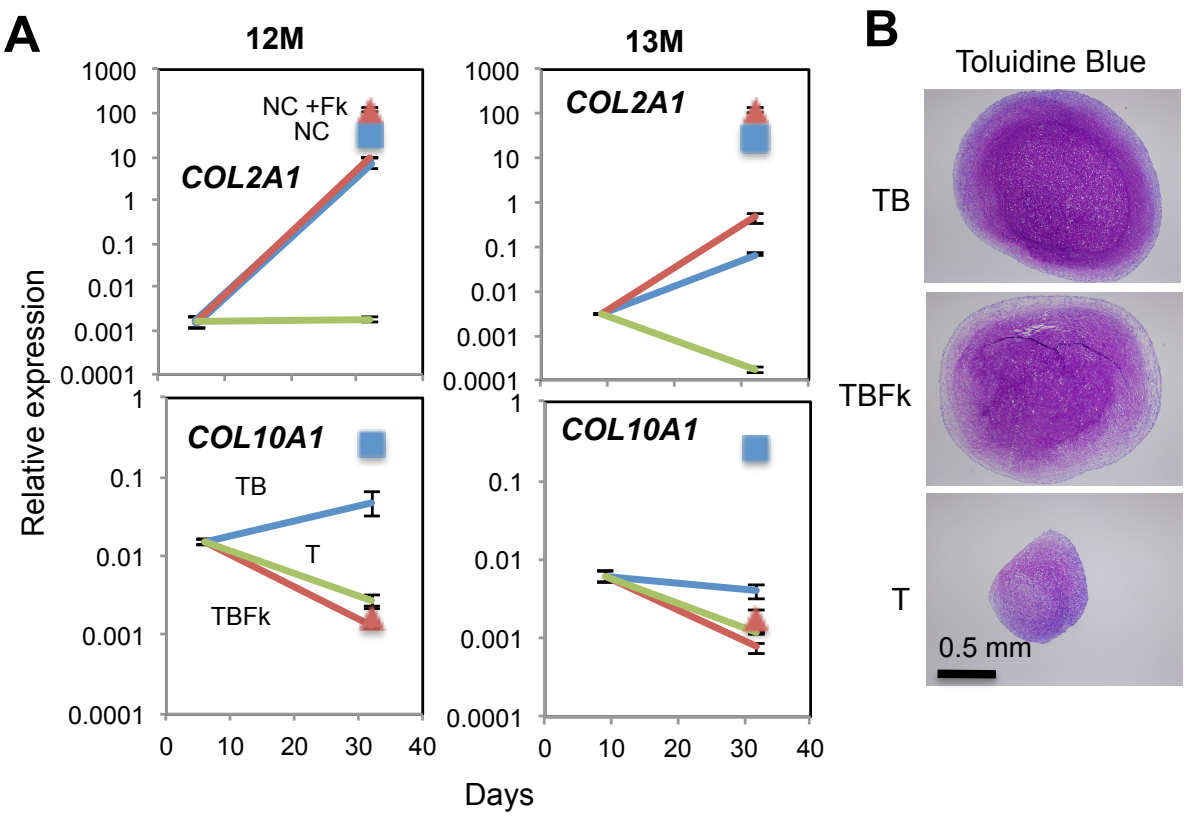

Fig. S5 Forskolin effects on chondrogenesis from dedifferentiated adult human nasal chondrocytes.

(**A**) Nasal chondrocytes from 2 male patients (12M, 13M) were individually differentiated in the presence of TGFβ alone (T) as described (Pelttari et al., 2014), or under modified conditions (TB: TGFβ+BMP4, and TBFk: TGFβ+BMP4+forskolin). On days 6 and 32, cartilage pellets were harvested and subjected to real-time RT-PCR. Supplementary to Fig. 4E. Blue square (NC): cartilage from hESC-ectomesenchymal cells formed under PTB (PDGF+TGFβ+BMP4), Brown triangle (NC+Fk): cartilage formed under PTBFk. (**B**) Supplementary to Fig. 4F. Toluidine blue (sGAG) staining of the same cartilage pellet samples.

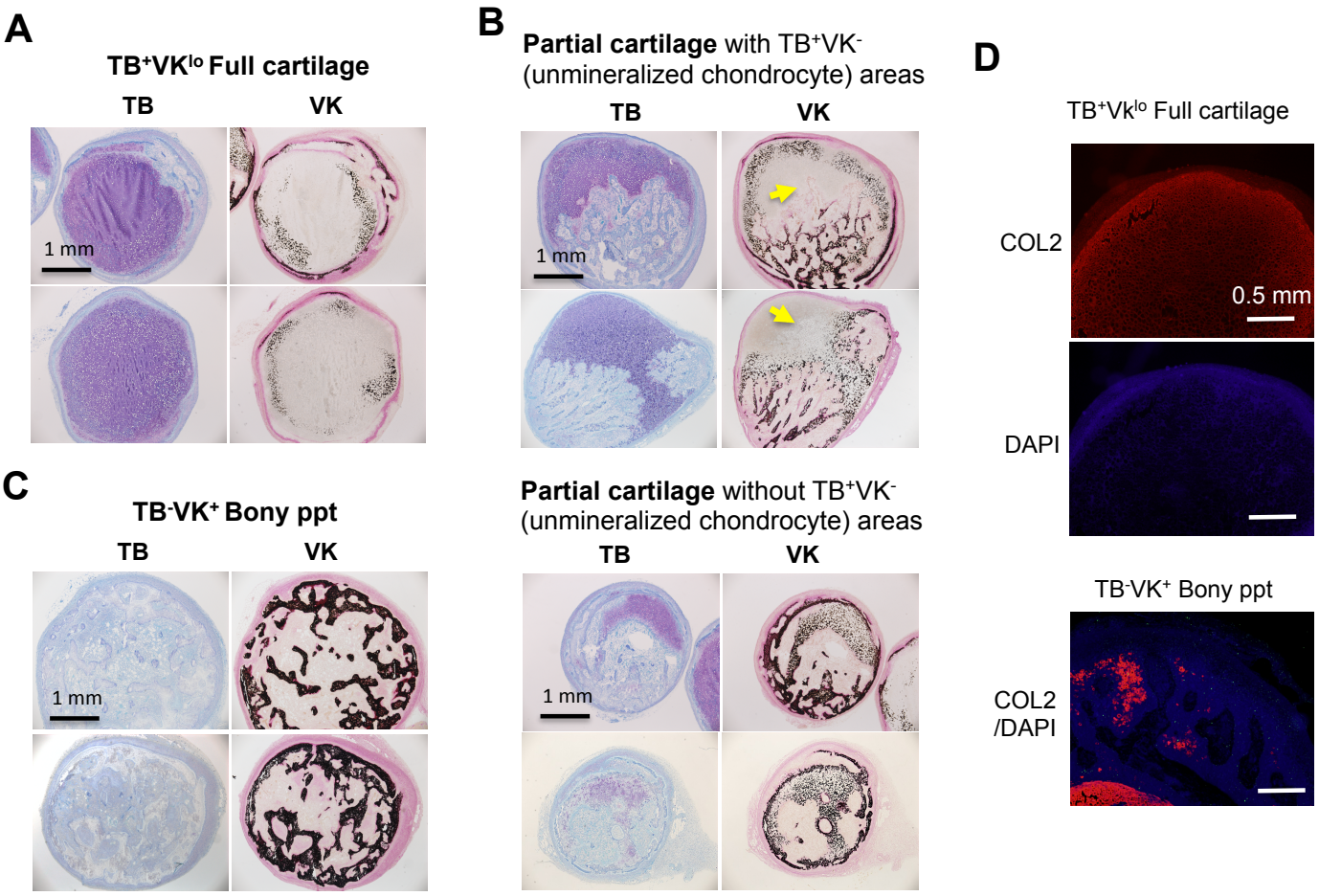

Fig. S6 Types of cartilage recovered from the 8-week ectopic transplantation.
(**A**) $TB^{+}VK^{lo}$ full cartilage: >80% area (usually the periphery of cartilage pellets did not stain) shows metachromatic (pink-purple) staining with Toluidine blue (TB) and consists largely of unmineralized chondrocytes. However, pellets often contained some mineralized chondrocytes that stained weakly with von Kossa (VK). (**B**) Partial cartilage containing bony area and cartilaginous area. Upper panel: The cartilaginous area contains groups of unmineralized chondrocytes (yellow arrows). Lower panels: The cartilaginous area contains mostly mineralized chondrocytes. (**C**) $TB^{-}VK^{+}$ bony pellet (ppt): Mostly consisting of bony areas stained densely with VK, often containing $TB^{-}VK^{-}$ marrow-like areas, but without TB^{+} cartilaginous area. (**A-C**) Supplementary to Fig. 6B. (**D**) Lower magnification (using x4 objective lens) photos of the immunofluorescence staining of the Fig. 6C post-transplantation pellets.

A

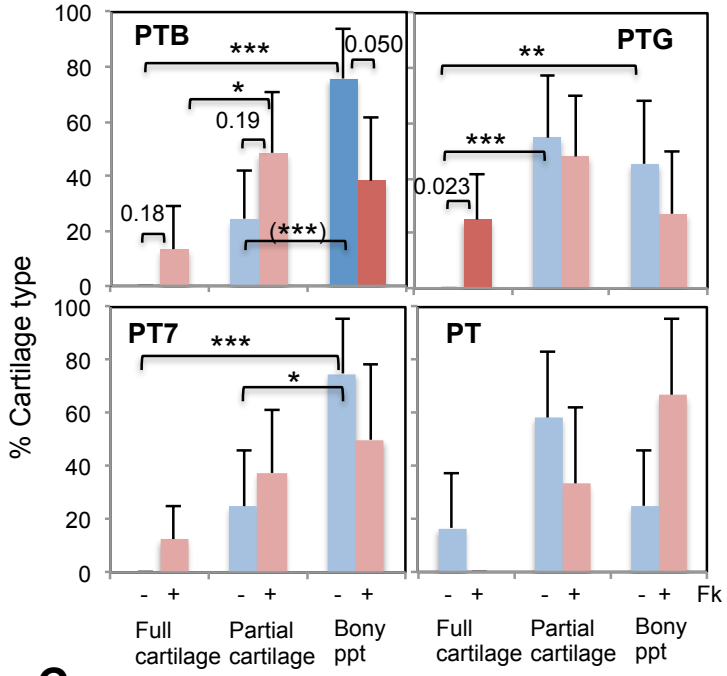

B

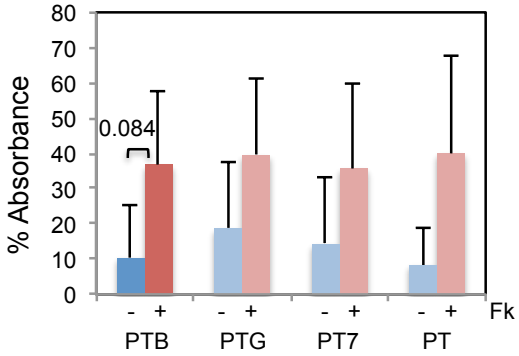

C

Ppt culture condition	$TB^{+}VK^{lo}$ Full cartilage (% viable ppts)	Partial cartilage (% viable ppts)	$TB^{-}VK^{+}$ Bony ppt (% viable ppts)	Recovered (viable) ppts	Absorbed ppts (% total ppts)	Transplanted (total) ppts
PTB	0 (0)	5 (24)	16 (76)	21	3 (13)	24
PTBFk	2 (12)	8 (47)	7 (41)	17	8 (32)	25
PTG	0 (0)	6 (36)	7 (64)	13	3 (19)	16
PTGFk	5 (36)	6 (43)	5 (21)	16	7 (30)	23
PT7	0 (0)	2 (25)	6 (75)	8	3 (27)	11
PT7Fk	2 (25)	3 (38)	3 (38)	8	3 (27)	11
PT	1 (14)	5 (57)	2 (29)	8	1 (11)	9
PTFk	0 (0)	1 (33)	2 (67)	3	4 (57)	7

D

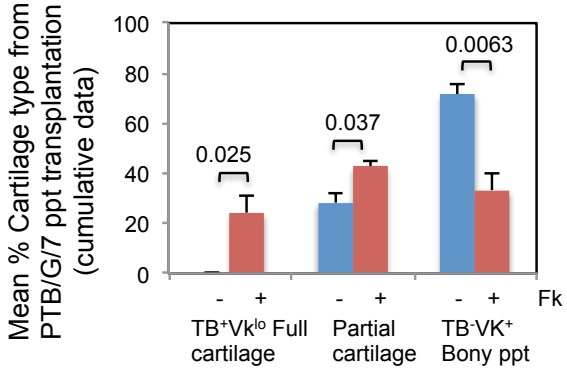

E

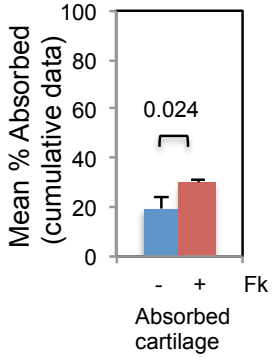

Fig. S7 Post-transplantation cartilage phenotypes:
Statistical analyses.
(**A**) Recovery of each of $TB^{+}VK^{lo}$ full cartilage, partial cartilage, and $TB^{-}VK^{+}$ bony pellet (ppt) after the 8-week ectopic transplantation of forskolin (Fk)-treated (Brown) and untreated (Blue) cartilage pellets was averaged and plotted with corresponding SEM and *P*-value (+/-Fk comparison, values of *P*>0.2 are not shown). PTB (PDGF+TGFβ+BMP4): n=9-10. PTG (PDGF+TGFβ+GDF5): n=7-8, PT7 (PDGF+TGFβ+BMP7): n=5-6, PT (PDGF+TGFβ): n=3-6. Other comparisons: PTB: **P*=0.060, ****P*=9.1E-07, $^{(***)}$*P*=0.0032, PTG: ***P*=0.023, ****P*=0.0082, PT7: **P*=0.065, ****P*=0.0014. Supplementary to Fig. 6D. (**B**) Pellet loss after the 8-week ectopic transplantation from each transplantation experiment was averaged and plotted with corresponding SEM and *P*-values (+/-Fk comparison). Supplementary to Fig. 6D.
Cumulative data analyses.
(**C**) The number of recovered $TB^{+}VK^{lo}$ full cartilage, partial cartilage, and $TB^{-}VK^{+}$ bony pellets (ppts) as well as the number of absorbed pellets after the 8-week ectopic transplantation of forskolin (Fk)-treated (Brown) and untreated (Blue) cartilage pellets were summed. Supplementary to Fig. 6D. (**D**) The % Full cartilage, % Partial cartilage and % Bony pellet (ppt) values from transplanted pellets produced under PTB (PDGF+TGFβ+BMP4), PTG (PDGF+TGFβ+GDF5) and PT7 (PDGF+TGFβ+BMP7) conditions, and those from PTB+Fk (PTBFk), PTGFk and PT7Fk conditions, shown in (**C**) were averaged and plotted with SEM with *P*-values. Supplementary to Fig. 6E **(E**) The % absorbed pellet values from transplanted pellets produced under PTB, PTG and PT7 conditions and those from PTBFk, PTGFk and PT7Fk conditions, shown in (**C**) were also averaged and plotted with SEM and *P*-value. Supplementary to Fig. 6E.

2. SUPPLEMENTAL TABLES

Table S1. Top GO Terms (Biological Process) *P*<1.0E-10

Top 20	Gene set names	P	FDR q
Fk induced genes	**（PTBFk＞PTB）**		
GO:0007059	chromosome segregation	5.71E-17	8.86E-13
GO:0098813	nuclear chromosome segregation	5.86E-17	4.54E-13
GO:0000819	sister chromatid segregation	1.57E-16	8.11E-13
GO:0007275	multicellular organism development	1.89E-16	7.31E-13
GO:0048856	anatomical structure development	3.10E-16	9.61E-13
GO:0032502	developmental process	6.38E-16	1.65E-12
GO:0048731	system development	1.06E-15	2.34E-12
GO:0032501	multicellular organismal process	3.09E-15	5.98E-12
GO:0000280	nuclear division	8.68E-15	1.49E-11
GO:0000278	mitotic cell cycle	1.25E-14	1.94E-11
GO:0051301	cell division	1.26E-14	1.77E-11
GO:0048285	organelle fission	3.94E-14	5.09E-11
GO:0022402	cell cycle process	7.15E-14	8.53E-11
GO:1903047	mitotic cell cycle process	1.26E-13	1.40E-10
GO:0007049	cell cycle	2.13E-13	2.20E-10
GO:0000070	mitotic sister chromatid segregation	7.61E-13	7.37E-10
GO:0140014	mitotic nuclear division	7.86E-13	7.17E-10
GO:0051239	regulation of multicellular organismal process	6.59E-12	5.67E-09
GO:0009790	embryo development	1.16E-11	9.48E-09
GO:0009653	anatomical structure morphogenesis	1.85E-11	1.44E-08
Fk suppressed genes	**（PTB＞PTBFk）**		
GO:0048731	system development	1.66E-17	2.57E-13
GO:0007275	multicellular organism development	2.57E-17	1.99E-13
GO:0048856	anatomical structure development	3.92E-16	2.02E-12
GO:0009888	tissue development	1.76E-15	6.83E-12
GO:0032502	developmental process	3.88E-15	1.2E-11
GO:0032879	regulation of localization	1.04E-12	2.7E-09
GO:0032501	multicellular organismal process	1.36E-12	2.64E-09
GO:0048513	animal organ development	2.26E-12	3.9E-09
GO:0007154	cell communication	3.71E-12	5.75E-09
GO:0050793	regulation of developmental process	6.68E-12	7.97E-09
GO:0051239	regulation of multicellular organismal process	7.03E-12	7.78E-09
GO:0009653	anatomical structure morphogenesis	1.1E-11	1.0E-08

GO:0023052	signaling	4.25E-11	3.66E-08

Table S2. Tissue/cell development-related GO Terms P<1.0E-04

Developmental GO	Gene set names	P	FDR q
Fk induced genes	**（PTBFk＞PTB）**		
GO:0007399	nervous system development	4.12E-10	2.56E-07
GO:0035295	tube development	2.46E-07	5.69E-05
GO:1901342	regulation of vasculature development	3.42E-07	7.70E-05
GO:0048514	blood vessel morphogenesis	3.62E-07	7.90E-05
GO:0001525	angiogenesis	5.80E-07	1.15E-04
GO:0045765	regulation of angiogenesis	8.33E-07	1.17E-04
GO:0022414	reproductive process	2.14E-06	3.29E-04
GO:0000003	reproduction	2.17E-06	3.31E-04
GO:0001568	blood vessel development	2.85E-06	4.06E-04
GO:0001655	urogenital system development	2.98E-06	4.12E-04
GO:0051960	regulation of nervous system development	4.03E-06	5.26E-04
GO:0001944	vasculature development	6.68E-06	8.04E-04
GO:0022008	neurogenesis	6.72E-06	8.02E-04
GO:0001501	skeletal system development	7.19E-06	8.45E-04
GO:0048699	generation of neurons	1.05E-05	1.16E-03
GO:0072358	cardiovascular system development	1.29E-05	1.39E-03
GO:0048608	reproductive structure development	1.73E-05	1.81E-03
GO:0061458	reproductive system development	1.98E-05	2.02E-03
GO:2000181	negative regulation of blood vessel morphogenesis	2.72E-05	2.58E-03
GO:0072001	renal system development	3.41E-05	3.10E-03
GO:0001822	kidney development	3.81E-05	3.36E-03
GO:1901343	negative regulation of vasculature development	4.86E-05	4.12E-03
GO:0061448	connective tissue development	5.54E-05	4.64E-03
GO:0001657	ureteric bud development	8.18E-05	6.58E-03
GO:0051216	cartilage development	8.56E-05	6.64E-03
GO:0060429	epithelium development	8.84E-05	6.72E-03
GO:0072164	mesonephric tubule development	9.00E-05	6.78E-03
GO:0072163	mesonephric epithelium development	9.00E-05	6.74E-03
GO:0046546	development of primary male sexual characteristics	9.10E-05	6.78E-03
Fk suppressed genes	**（PTB＞PTBFk）**		
GO:0048699	generation of neurons	2.54E-09	1.31E-06
GO:0022008	neurogenesis	1.51E-08	6.31E-06
GO:0030182	neuron differentiation	3.11E-08	1.18E-05
GO:0001503	ossification	7.79E-08	2.42E-05

GO:0060537	muscle tissue development	1.45E-07	4.24E-05
GO:0007399	nervous system development	2.01E-07	5.37E-05
GO:0014706	striated muscle tissue development	2.16E-07	5.68E-05
GO:0060429	epithelium development	3.02E-07	7.31E-05
GO:0072001	renal system development	3.90E-07	8.77E-05
GO:0007517	muscle organ development	4.02E-07	8.78E-05
GO:0072359	circulatory system development	5.47E-07	1.10E-04
GO:0001501	skeletal system development	6.34E-07	1.24E-04
GO:0001822	kidney development	1.44E-06	2.56E-04
GO:0030278	regulation of ossification	1.76E-06	2.90E-04
GO:0035239	tube morphogenesis	1.98E-06	3.21E-04
GO:0060562	epithelial tube morphogenesis	2.41E-06	3.81E-04
GO:0001655	urogenital system development	2.84E-06	4.27E-04
GO:0045664	regulation of neuron differentiation	4.50E-06	6.34E-04
GO:0016202	regulation of striated muscle tissue development	4.65E-06	6.44E-04
GO:0061061	muscle structure development	4.99E-06	6.84E-04
GO:1901861	regulation of muscle tissue development	5.54E-06	7.47E-04
GO:0035295	tube development	6.06E-06	7.90E-04
GO:0048514	blood vessel morphogenesis	6.14E-06	7.86E-04
GO:0048634	regulation of muscle organ development	6.59E-06	8.30E-04
GO:0051960	regulation of nervous system development	9.35E-06	1.08E-03
GO:0003007	heart morphogenesis	1.07E-05	1.21E-03
GO:0045165	cell fate commitment	1.20E-05	1.35E-03
GO:0001649	osteoblast differentiation	1.40E-05	1.51E-03
GO:0031214	biomineral tissue development	1.81E-05	1.90E-03
GO:0007507	heart development	1.90E-05	1.97E-03
GO:0050767	regulation of neurogenesis	2.24E-05	2.23E-03
GO:0001568	blood vessel development	2.66E-05	2.58E-03
GO:0048641	regulation of skeletal muscle tissue development	3.00E-05	2.87E-03
GO:0048666	neuron development	3.48E-05	3.20E-03
GO:0060348	bone development	3.93E-05	3.48E-03
GO:2000725	regulation of cardiac muscle cell differentiation	4.48E-05	3.88E-03
GO:0001525	angiogenesis	4.48E-05	3.86E-03
GO:0055024	regulation of cardiac muscle tissue development	5.34E-05	4.38E-03
GO:0048738	cardiac muscle tissue development	5.84E-05	4.74E-03
GO:0001944	vasculature development	7.16E-05	5.64E-03
GO:2000726	negative regulation of cardiac muscle cell differentiation	8.15E-05	6.28E-03
GO:0030509	BMP signaling pathway	8.82E-05	6.71E-03

Table S3. Fk-induced gene list.

Skeletogenesis-related genes	PTB DESeq	PTBFk DESeq	fold induction by Fk ≥2.0	FDR adjusted P<0.05
DLK1	15532.21	50776.97	3.27	7.04E-09
MMP2	7223.26	24243.16	3.36	7.85E-08
CILP2	9466.24	19658.75	2.08	4.22E-05
SFRP5	1947.04	6689.51	3.44	4.86E-02
SFRP1	1206.22	4896.12	4.06	1.84E-07
PBX3	2120.04	5234.18	2.47	2.55E-16
RUNX1	1278.92	3929.79	3.07	7.03E-16
PTN	697.46	2631.56	3.77	5.87E-08
TNFRSF11B	1198.53	2595.39	2.17	7.90E-03
SOX11	1244.26	2500.55	2.01	6.39E-07
SIX2	857.18	2380.29	2.78	2.34E-10
CITED2	879.18	2051.24	2.33	3.60E-09
GATA3	887.45	1870.27	2.11	2.18E-03
ALX4	648.05	1803.80	2.78	2.77E-10
EYA1	517.90	1625.08	3.14	9.49E-15
FAP	407.94	1371.01	3.36	4.16E-02
INHBA	370.15	1321.50	3.57	4.34E-07
ITGA4	765.55	2255.70	2.95	5.45E-11
GATA2	254.42	747.22	2.94	1.06E-03
SOCS3	317.62	695.17	2.19	1.87E-02
RSPO3	50.16	597.70	11.94	9.85E-23
TGFBR3	56.25	377.66	6.73	1.03E-10
RSPO2	59.30	202.07	3.42	1.24E-02
LHX8	74.28	152.34	2.04	1.84E-02
CSF3R	6.60	77.04	11.63	8.39E-05
UCMA	1.60	68.10	43.15	1.03E-06
LHX6	15.71	45.90	2.90	4.81E-02
DACT2	1.83	21.03	11.19	1.65E-03
RARRES1	3.65	15.40	4.20	2.71E-02
DLL4	0.29	8.27	24.42	2.23E-02
BMP signaling genes	**PTB** DESeq	**PTBFk** DESeq	**fold induction by Fk ≥2.0**	**FDR adjusted P<0.05**
GREM1	1346.97	4501.42	3.34	4.40E-08
GDF5	69.95	159.11	2.28	5.66E-04
BMP5	38.96	120.17	3.09	2.66E-02
CHRDL2	11.44	83.24	7.23	3.41E-09
BMPER	5.65	32.00	5.82	2.57E-03

Cell cycle control genes	PTB DESeq	PTBFk DESeq	fold induction by Fk ≥2.0	FDR adjusted P<0.05
CCNB1	336.49	690.73	2.06	1.64E-02
CCNA2	236.81	592.52	2.51	1.00E-02
CDK1	166.77	584.12	3.51	2.22E-02
CDK18	144.72	465.27	3.21	2.62E-04
CCNB2	113.80	287.64	2.54	7.50E-04
E2F1	101.41	232.61	2.30	1.41E-03
CCNE2	47.18	105.64	2.23	3.27E-03
MYCN	26.06	95.27	3.63	8.36E-03
CDC45	22.95	55.67	2.45	9.40E-03
CDC25C	14.73	47.28	3.24	2.20E-02
E2F8	11.04	41.65	3.82	6.59E-03
CCNA1	4.44	19.91	4.50	8.17E-03
DNA replication genes	**PTB** DESeq	**PTBFk** DESeq	**fold induction by Fk ≥2.0**	**FDR adjusted P<0.05**
ORC6	94.27	190.00	2.02	2.50E-02
MCM10	43.79	125.85	2.88	1.17E-02
CDT1	46.94	109.89	2.35	5.77E-03
ORC1	30.51	75.11	2.47	5.11E-03

Table S4. Fk-suppressed gene list.

Skeletogenesis-related genes	PTB DESeq	PTBFk DESeq	fold suppression by Fk ≥2.0	FDR adjusted P<0.05
COL10A1	759335.21	27191.44	27.93	1.42E-11
PTH1R	57556.05	20996.49	2.74	1.25E-07
CYTL1	20403.47	6378.10	3.20	4.21E-02
MEF2C	19516.42	8279.90	2.36	8.25E-05
IHH	16969.11	3656.91	4.64	1.10E-03
IBSP	16004.16	85.41	187.55	4.17E-09
IGF1R	13863.53	5317.81	2.61	1.57E-33
NRCAM	7953.61	1665.61	4.78	1.15E-03
GSK3B	6291.89	2568.07	2.45	1.92E-17
RUNX2	5022.87	1617.64	3.11	2.93E-06
ALPL	4578.90	152.96	29.96	5.13E-09
FST	4174.02	953.38	4.38	3.21E-03
SP7	3828.53	646.53	5.92	3.31E-10
FOXA2	3504.24	994.51	3.52	1.53E-11
IRX5	2042.96	310.43	6.59	1.03E-10
CD24	2006.71	213.78	9.40	3.49E-05
WNT5B	1648.18	610.88	2.70	3.62E-07
DKK1	1516.17	64.48	23.42	1.04E-07
WNT11	1479.72	363.90	4.06	5.93E-08
VDR	1478.11	428.00	3.45	6.62E-12
VAV3	1406.94	97.05	14.52	8.08E-07
DLX5	1256.06	593.71	2.12	1.29E-02
WNT16	1914.44	290.74	6.58	7.95E-03
IL17B	1070.22	43.11	24.66	4.55E-35
JAG2	896.56	430.89	2.08	1.49E-08
COL4A6	759.47	116.31	6.55	2.48E-16
SPP1	755.78	21.22	35.38	6.60E-06
DACH1	529.83	41.79	12.84	9.47E-15
AXIN2	328.09	154.90	2.12	1.15E-03
DLL1	310.31	45.14	6.94	2.20E-09
KL	191.59	62.53	3.05	1.18E-05
MEPE	187.06	1.02	186.09	9.20E-16
CUX2	175.05	0.79	232.46	2.60E-16
ANK1	141.71	8.88	16.55	7.71E-12
WNT10B	138.31	22.82	6.05	2.43E-09
DLX3	93.87	26.88	3.55	1.15E-04
DKK2	63.92	7.89	7.96	1.58E-02
DMP1	46.19	9.41	4.77	2.58E-02

MYOCD	28.52	3.55	8.39	9.44E-04
CYSLTR1	24.29	0.00	127.12	4.72E-06
DCX	16.86	3.81	4.30	1.86E-02
CALCRL	13.48	0.75	17.85	2.52E-03
BMP signaling genes	**PTB** DESeq	**PTBFk** DESeq	**fold suppression by Fk ≥2.0**	**FDR adjusted P<0.05**
DCN	27128.19	13080.70	2.07	2.15E-02
SMPD3	5685.56	308.89	18.41	1.22E-06
ID2	2699.09	1246.36	2.16	5.73E-07
BMP2	2153.56	540.41	3.99	6.72E-11
CHRDL1	411.70	189.02	2.18	9.14E-11
BMP8A	254.56	105.41	2.43	5.90E-04
BMP8B	34.98	10.06	3.51	1.98E-02
Cell cycle control genes	**PTB** DESeq	**PTBFk** DESeq	**fold suppression by Fk ≥2.0**	**FDR adjusted P<0.05**
CDKN1A	8873.45	3582.71	2.48	1.50E-16
CDC42EP3	3631.13	1647.02	2.21	1.93E-05
MYCL	34.37	11.45	2.95	1.15E-02
DNA replication genes	**PTB** DESeq	**PTBFk** DESeq	**fold suppression by Fk ≥2.0**	**FDR adjusted P<0.05**

Table S5. Comparative bioinformatics analysis between Fk-induced genes with Wu, et al.'s human embryonic chondrocytes.

Fk-induced (fold induction ≥2.0) genes	17w articular chondrocytes Microarray unit	6w condensing chondrocytes Microarray unit	17w > 6w (fold increase >1.75)
ST6GALNAC3	9.51	4.05	2.34
LIX1	18.04	9.49	1.90
MXRA5	11.42	6.12	1.87
CENPK	8.70	4.70	1.85
KIT	7.51	4.09	1.84
JAKMIP2	13.90	7.66	1.81
BAI3	12.07	6.87	1.76

Fk-induced (fold induction ≥2.0) genes	17w articular chondrocytes Microarray unit	6w condensing chondrocytes Microarray unit	17w < 6w (fold increase >1.75)
CHI3L2	4.97	11.54	2.32
ICAM1	16.76	38.67	2.31
SERPINA3	5.28	12.02	2.28
ITIH6	4.25	9.19	2.16
BHLHE40	10.85	23.16	2.14
C1S	9.30	19.58	2.11
NNMT	4.67	9.74	2.08
GPRC5A	15.35	31.18	2.03
TRAF1	9.15	18.47	2.02
TNFRSF11B	11.07	21.75	1.96
PLA2G2A	6.35	11.88	1.87
ATP6V0A4	5.74	10.58	1.84
OSMR	17.59	31.94	1.82
INSC	4.31	7.61	1.77
CST1	4.07	7.14	1.76

Table S6. Comparative bioinformatics analysis between Fk-suppressed genes with Wu, et al.'s human embryonic chondrocytes.

Fk-suppressed (fold reduction ≥2.0) genes	17w articular chondrocytes Microarray unit	6w condensing chondrocytes Microarray unit	17w > 6w (fold increase >1.75)
DKK1	8.76	3.55	2.47
DACH1	23.78	10.05	2.37
CDH10	7.35	3.24	2.27
DCX	18.47	9.52	1.94
FGF13	10.04	5.67	1.77
GPR64	9.31	5.32	1.75

DKK1 and *DCX* are articular cartilage genes.
Forskolin suppresses the expression of these articular cartilage genes.

Fk-suppressed (fold reduction ≥2.0) genes	17w articular chondrocytes Microarray unit	6w condensing chondrocytes Microarray unit	17w < 6w (fold increase >1.75)
AGT	3.15	13.09	4.15
ISG20	9.61	25.49	2.65
AOC3	3.57	7.21	2.02
SLC28A3	7.26	14.12	1.95
PPP4R4	11.89	21.47	1.81
LOC100126784	13.15	23.57	1.79

Table S7. n (independent experiment number) and *P*-value lists.

Gene	*P*, n	*P* and n values for each condition		
Fig. 2B		**PTBFk/PTB**	**PTGFk/PTG**	**PT7Fk/PT7**
COL2A1	*P*	0.10	0.28	0.17
	n	10	8	6
COL10A1	*P*	5.4E-21	1.1E-08	4.1E-10
	n	17	11	9
COL1A1	*P*	2.5E-03	1.7E-04	6.3E-03
	n	7	7	6
ALPL	*P*	8.6E-04	0.016	0.57
	n	6	3	3
SOX9	*P*	0.32	0.26	0.20
	n	9	3	3
RUNX2	*P*	1.9E-06	0.0097	0.14
	n	10	3	3
BMP4	*P*	0.0081	0.0017	1.0E-04
	n	3	3	3
MMP13	*P*	0.12	0.68	0.63
	n	3	3	3
Fig. 3B Left		**+cAMP/-cAMP**	**+Fk/-Fk**	**+IBMX/-IBMX**
COL2A1	*P*	0.35	0.037	0.30
	n	8	10	8
COL10A1	*P*	9.3E-06	7.9E-09	4.2E-05
	n	6	8	8
Fig. 3B Right		**+Fk/-Fk**	**+C59/-C59**	**+Fk+C59/-Fk-C59**
COL2A1	*P*	0.28	0.36	0.35
	n	5	6	6

COL10A1	*P*	5.9E-06	0.0077	1.8E-06
	n	5	6	6
	P	0.0031		

3. SUPPLEMENTAL EXPERIMENTAL PROCEDURES

Human pluripotent stem cell culture.

H9 hESCs were maintained on mouse embryonic fibroblast feeder cells in SR medium: Dulbecco's modified Eagle's medium (DMEM): Ham's F12 (1:1), 20% (v/v) KnockOut Serum Replacement (KSR), 2 mM GlutaMAX, 0.1 mM non-essential amino acids (all from Invitrogen, Carlsbad, CA) and 90 μM β-mercaptoethanol (Sigma-Aldrich, St. Louis, MO), supplemented with 4 ng/ml FGF2 (hFGF2-IS, Miltenyi Biotec, Bergisch Gladbach, Germany) as described (Umeda et al., 2012), Alternatively CY2-SOX9-2A-ZsGreen-2A-Puro (SOX9-GFP) hiPSCs derived from the former Center for Regenerative Medicine in NIH were maintained in Essential-8 medium on a vitronectin-coated plate (Invitrogen). Media and supplements, buffers and specialized tissue culture plates were generally sourced as described (Umeda et al., 2015; Umeda et al., 2012; Wang and Nakayama, 2009; Wang et al., 2010).

Generation and expansion of ectomesenchymal cells from hPSCs through neural crest specification.

Human PSCs were treated with collagenase I (Worthington, Lakewood, NJ) to generate clumps, which were plated onto a low-adhesion dish (Sarstedt, Nümbrecht, Germany) and cultured for 1 day in a chemically defined medium (CDM): Iscove's modified Dulbecco's Medium (IMDM) (Sigma): Ham's F12 (Invitrogen) (1:1), 0.5% (w/v) bovine serum albumin (Sigma), 1% (v/v) synthetic lipid concentrate (Invitrogen), 100 μg/ml human holo-transferrin (Sigma), 20 μg/ml human insulin (Sigma), 0.17 mM ascorbic acid-2-phosphate (AA2P, Sigma), 2 mM GlutaMAX (Invitrogen), and 0.4 mM monothioglycerol (MTG, Sigma), supplemented with 10 μM SB431542 (Tocris) and 5 μM Y27632 (ROCK inhibitor, Tocris, Ellisville MO) at 37^{o}C under 5% CO_2/5% O_2. The embryoid bodies (EBs) formed were transferred to a plate coated with 0.1% (w/v) porcine gelatin (Sigma) on day 1 and cultured in CDM with 10 μM SB431542 and 2 μM CHIR99021 (Tocris) till day 5. Then media was changed to CDM with 10 μM SB431542 only. On the day of

harvest (usually day 6), a suspension of single cells was prepared using TrypLE Select (Invitrogen), diluted 2.5-fold with 0.5 mM EDTA in D-PBS (without Ca^{2+} and Mg^{2+}), immunostained with the AlexaFluor647-conjugated mouse anti-hCD271 (#560326, BD Biosciences, San Jose, CA) and phycoerythrin (PE)-conjugated mouse anti-hCD73 (#344004, BioLegend, San Diego, CA) monoclonal antibodies, and the $CD271^{hi}CD73^{-}$ cell population was isolated by FACS as described (Umeda et al., 2015). Alternatively, the $CD271^{hi}$ cell population was isolated by magnetic cell sorting using the MACS cell separation system and CD271 microbead kits (#130-092-283, Miltenyi Biotec). The sorted cells were transferred to a plate coated with 10 μg/ml human fibronectin (Sigma) and cultured overnight at 4°C in CDM supplemented with 2 μg/ml heparin (Sigma), 2.5 μg/ml catalase (Sigma), 5-10 ng/ml FGF2 and 5-7.5 μM SB431542 (FSb medium), at 37°C under 5% CO_2/5% O_2. The cells were passaged every 2-3 days at 3-4 x 10^4 cells/cm^2 using the diluted TrypLE Select as described (Umeda et al., 2015). At the desired density, the ectomesenchymal cells were primed with CDM supplemented with 5 ng/ml FGF2 and 10 ng/ml TGFβ3 (hTGFβ3, R&D Systems, Minneapolis, MN) for 3 days prior to chondrogenesis induction, and harvested with TrypLE Select.

Generation and isolation of paraxial mesoderm from hPSCs.

Human PSCs were differentiated 3-dimensionally using the CDM-based EB-forming culture as described (Umeda et al., 2015; Umeda et al., 2012) with slight modifications. Briefly, the EB culture was initiated in the CDM with extra anti-oxidants: 2.5 μg/ml catalase, 1.5 μg/ml reduced glutathione (Sigma) and 5 mM proline (Sigma) (CDM-AO medium), supplemented with 5 μM Y27632, 5 ng/ml BMP4 (hBMP4, R&D), and 5 μM CHIR99021, and maintained at 37°C under 5% CO_2/5% O_2. On day 1, medium was changed to CDM-AO containing 5 μM CHIR99021. On day 2, 100-500 ng/ml Noggin (mNoggin-Fc, R&D) was added. On day 3, EBs were transferred to CDM-AO containing 0.9% (w/v) methylcellulose (Methocel A4M, Dow Chemical, Midland, MI) with 100 ng/ml Noggin, 0.5-2 μM CHIR99021, 0.2 μM PD173074 (FGFR1 inhibitor, Tocris), 3

μM SB431542 and 5 ng/ml PDGF (hPDGF-BB, R&D). On day 6 or 7, single EB cells were obtained by treatment of EBs with the diluted TrypLE Select for 3-5 min at 37°C. The cells were stained with mouse anti-hPDGFRα (IgG_{2a}, #556001, BD) and anti-KDR (IgG_1, #101-M20 ReliaTech, Wolfenbüttel, Germany) monoclonal antibodies, then with biotin-conjugated goat anti-mouse IgG_{2a} (#1080-08), and PE-conjugated goat anti-mouse IgG_1 antibodies (#1070-01) from SouthernBiotech (Birmingham, AL), and finally with allophycocyanin (APC)-conjugated streptavidin (#554067, BD). The $KDR^-PDGFR\alpha^+$ cell population was isolated by FACS as described (Umeda et al., 2012).

Expansion of hPSC-derived paraxial mesoderm cells.

The FACS-isolated cells were cultured on a fibronectin coated plate in CDM supplemented with 2 μg/ml heparin, 2.5 μg/ml catalase, 5-10 ng/ml FGF2, 5-10 ng/ml PDGF, 5-7.5 μM SB431542 and 2 μM CHIR99021 (FPSbC medium), at 37°C under 5% CO_2/5% O_2 and passaged every 2-3 days at 3.0 x 10^4 cells/cm^2 using the diluted TrypLE Select. At passage 2, the medium composition was changed to FSbC by removal of PDGF from the FPSbC medium.

Expansion of human adult nasal chondrocytes.

Human adult nasal chondrocytes from one female (11F) and two male patients (12M, 13M) were independently isolated as described (Centola et al., 2013). Expansion of the chondrocytes was performed in DMEM (high glucose), 0.1 mM non-essential amino acids, 1 mM sodium pyruvate, 25 mM HEPES buffer, 2 mM GlutaMAX (all from Invitrogen) supplemented with 5% (v/v) fetal bovine serum (FBS, Hyclone, Logan, UT), 5 ng/ml FGF2 and 1 ng/ml hTGFβ1 (R&D), at 37°C under 5% CO_2 for up to passage 3.

Scaffold-free cartilage formation: pellet culture.

To induce chondrogenesis from hPSC-derived chondroprogenitors, aliquots of 2-3×10^5 cells were centrifuged in a 15-ml conical tube (BD) to form pellets, and cultured in a 0.5 ml of serum-free chondrogenic media: DMEM (high glucose), 1 mM sodium pyruvate, 1% (v/v) ITS+ (BD),

100 nM dexamethasone (Sigma), 0.17 mM AA2P, 0.35 mM proline, 2 mM GlutaMAX, and 50 μM MTG, supplemented with 40 ng/ml PDGF. On day 6 of pellet culture, 10 ng/ml TGFβ3 was added, and on day 10, a BMP (hBMP4 [PTB condition], hGDF5 [PTG condition], or hBMP7 [PT7 condition], all from R&D) was added at 50 ng/ml. For the dedifferentiated human nasal chondrocytes, chondrogenesis was initiated in the presence of 10 ng/ml TGFβ3 from day 0 as described (Pelttari et al., 2014). In some pellets, 50 ng/ml BMP4 was added on day 10. When necessary the following were added on day 11 or 12: the activator of adenylyl cyclase, forskolin, 3-30 μM (Tocris); canonical WNT signaling inhibitors such as KY02111, 10 μM, (Tocris) (Minami et al., 2012), and β-catenin-TCF interaction inhibitor (Gonsalves et al., 2011), iCRT14, 25 μM, (Tocris); general WNT signaling inhibitors such as the L-type calcium channel blocker that induces soluble WNT binding proteins (Takamatsu et al., 2014), verapamil, 50 μM, (Tocris), and a porcupine inhibitor that inhibits WNT secretion (Proffitt et al., 2013), Wnt-C59, 30-120 nM, (Cellagen Technology, San Diego, CA); and cGMP signaling inhibitors such as the cGMP-dependent protein kinase inhibitor that works at least *in vitro* (Burkhardt et al., 2000), KT5824, 4 μM, (Tocris) and a potent cGMP antagonist (Poppe et al., 2008), Rp-8-Br-PET-cGMPS, 30-60 μM, (Tocris). In separate experiments, the following were added on day 11 or 12: cAMP analogs such as the PKA activator, N^6-benzoyl-cAMP, 40-100 μM, (Tocris and EMD Millipore, Temecula, CA): an EPAC activator (Christensen et al., 2003; Poppe et al., 2008), 8-pCPT-2'-O-Me-cAMP-AM, 3-6 μM, (Tocris and Axxora, Farmingdale, NY); the non-specific phosphodiesterase inhibitor IBMX, 0.5 mM, (Tocris), and non/less-active version of forskolin, 1,9-dideoxyforskolin, 12.5-25 μM, (Tocris). The concentrations used were in a published range that had been successful for various cell-based assays. The pellet cultures were maintained at 37°C under 7.5% CO_2 for up to 40 days. When the cartilage pellet became large enough to fill the bottom of the conical tube (larger than 4 mm in diameter), the pellet was transferred to a well of a 24-well tissue culture-untreated plate (BD), and cultured in 1.0-1.5 ml of chondrogenic medium at 37°C

under 7.5% CO_2/5% O_2. Some cartilage pellets were then fixed with Zinc-Formalin (Z-Fix, American MasterTech, Lodi, CA) for 1 day, paraffin-embedded, sectioned (5 μm), deparaffinized, rehydrated, and stained with 0.1% (w/v) Toluidine Blue (Sigma).

Isolation of chondrocytes from cartilage pellets.

A cartilage pellet was treated with 0.3-0.5 ml of 4 mg/ml collagenase (D [Roche/Sigma]: XI [Sigma]=1:1 in DMEM) (Nakayama et al., 2000) at 37°C for 3 h with occasional shaking. Enzyme digestion was stopped by the addition of 1 ml DMEM, 10% (v/v) FBS. Pellets were dissociated with repetitive pipetting, and remaining aggregates were removed with a 40 μm mesh (BD). Cells were washed twice with an appropriate medium or solution. Approximately 1.5-5.0 x 10^5 cells were recovered per pellet.

EdU labeling of chondrocytes in cartilage pellets.

Ten to 20 μM of EdU (Click-iT Plus EdU AlexaFluor 647 Flow Cytometry Assay Kit, Invitrogen) was added to pellet cultures and maintained for 21-25 h. The labeling time was determined by test labeling of pellets for 3 h, 21 h, 3 days, and 7 days. Under PTB+/-Fk conditions, approximately 1 day of labeling gave the most reliable values of EdU^+ cell population from H9 hESC- and CY2 SOX9-GFP hiPSC-progeny-derived cartilage. Two to three cartilage pellets were combined, and single cells were isolated as described above. Cells were washed with PBS and subjected to brief fixation with para-formaldehyde, followed by permeabilization with saponin, and then to AlexaFluor 647-picolyl azide treatment, according to the manufacturer's recommendation. The labeled cells were analyzed by FACS LSRII (BD).

Isolation and quantification of DNA, RNA and sGAG from cartilage.

Cartilage pellets were collected and submerged in liquid N_2, manually cracked into small pieces with a liquid N_2 cooled mortar and a pellet pestle, and homogenized in the lysis buffer (RLT, Qiagen, Valencia, CA). The cleared lysates were then subjected to DNA, RNA and proteins isolation using the AllPrep DNA/RNA/Protein mini kit (Qiagen). The purified RNA was used for

real-time RT-PCR analysis. The isolated proteins were subjected to papain digestion for 20-24 h at 60^{o}C (125 μg/ml papain, 10 mM cysteine in sodium phosphate-EDTA pH 6.5 [all from Sigma]), and released sGAG was quantified by the 1,9-dimethyl methylene blue (DMMB [Sigma], 16 μg/ml in glycine-NaCl pH 3) serial-dilution assay, using bovine tracheal chondroitin-4-sulfate (Biocolor, UK) as standard. The OD590-530 was measured with SpectraMax M2 (Molecular Devices, Sunnyvale, CA). The DNA isolated with the AllPrep kit was quantified by the Hoechst33258 (Sigma, 0.2 μg/ml in Tris·HCl-EDTA-NaCl pH 7.5) serial-dilution assay, using bovine thymus DNA (Sigma) as standard. The fluorescence (emission 460 nm, excitation 360 nm) was measured with SpectraMax M2. The total sGAG and DNA amounts per particle, along with comparative ratios of the sGAG and DNA, were then calculated. Results are presented as mean values with SEM (the standard error of the mean) shown by thin error lines.

Gene expression profiling.

The isolated RNA was reverse transcribed (RT) using a Superscript III kit (Invitrogen) and real-time polymerase chain reaction (RT-PCR) was performed using the Taqman Gene Expression Assay and ABI7900 (Applied Biosystems, Foster City, CA). The expression levels of individual genes from duplicate or triplicate reactions were normalized against *EEF1A1* transcript ($2^{-\Delta Ct}$ x100) and averaged to obtain relative expression, as described (Wang and Nakayama, 2009). The RT-PCR results are presented as mean relative expression levels with SEM shown by the thin error lines. Undetectable levels of all the genes tested lie in the relative expression range of 0.001 to 0.0001. The "*% COL10A1/COL2A1"* is a relative expression of *COL10A1* normalized against that of *COL2A1* and multiplied by 100. The "Change in expression" was determined by the ratio of gene expression levels between treated (+) and untreated (-) pellets.

For RNA Sequencing analysis (RNA-seq), three independent sets of PTB pellets, and four independent sets of PTBFk pellets were prepared from passage 5-8 ectomesenchymal cells (i.e., FSb-expanded CD271^{hi}CD73^{-} neural crest-like progeny of H9 hESCs). On day 26-28

of pellet culture, 5 to 6 cartilage pellets were harvested, combined and total RNA was extracted with an RNeasy mini kit (Qiagen). Poly (A)-tailed messenger RNA was enriched using Poly(A)Purist Kit (Ambion, Foster City, CA) before the preparation of the RNA-seq library using an Ultra directional RNA library prep kit for Illumina (New England Biolabs, Ipswich, MA) per manufacturer's instructions. RNA-seq was performed using the Illumina Nextseq500 with the 150 bp pair-ended running mode. Sequencing reads were aligned against the GRCh37/hg19 reference genome using bowtie2 (Langmead and Salzberg, 2012) with default parameter. Only uniquely mapped reads were used for downstream analysis. HTseq was used to count the read numbers mapped to each gene. DESeq2 (Love et al., 2014) was used to call the significantly differentially expressed genes (fold change ≥2; false discovery rate ≤0.05) between two conditions. The normalized gene counts from DESeq2 was used to do the normalization. The analyzed data are summarized in Tables S1-4. Sequenced reads were deposited to GEO (Accession #: GSE116173).

Subcutaneous transplantation of cartilage particles.

In preparation for cartilage transplantation, 6-12-week-old female immunocompromized NSG mice (NOD.Cg-*Prkdc*^{scid} *Il2rg*^{tm1Wjl}/SzJ; Stock No: 005557) were anesthetized with isoflurane. After they had lost the pedal withdrawal reflex, buprenorphine was injected subcutaneously near the proposed site of incision, followed by clipping of back hair, skin disinfection with chlorhexidine and 70% (v/v) alcohol, and placement of a sterile drape around the area of incision. Mice were placed on a heated pad during the procedure to preserve body temperature. Two mid-longitudinal skin incisions of approximately 1 cm were made on the dorsal neck area of each mouse, and subcutaneous pockets formed by blunt dissection. *In vitro*-made cartilage pellets (of approximately 1-5 mm "wet" diameter) were individually placed into each pocket, with up to two transplants per mouse. Incisions were closed with skin adhesive. After 8 weeks, the transplanted mice were euthanized and cartilage pellets were harvested, fixed with Z-Fix for 4 days, embedded in plastic, sectioned (5 μm), deplastified, rehydrated and stained with von

Kossa counterstained with van Gieson, or with Toluidine Blue. Control experiments were performed using a piece of articular cartilage surface of 2-year-old bovine knee (4 mm in diameter x 2-3 mm in depth) obtained from Animal Technologies (Tyler, TX). The transplantation experiments were performed under the regulation of IACUC for the University of Texas Health Science Center at Houston (UTHealth).

Immunohistological staining.

The *in vitro*-made cartilage pellets were fixed with Z-Fix for 1 day, and paraffin embedded, sectioned (5 μm), deparaffinized with xylene, rehydrated, heat treated in the antigen-retrieval solution (Dako, Glostrup, Denmark), blocked with the blocking buffer (Dako), and subjected to immunofluorescence detection of COL1 (for detecting mesenchymal cells or osteoblasts), COL2 (for detecting chondrocytes), or Ki67 (for detecting proliferating cells). The sections of *in vivo*-derived, plastic-embedded cartilage pellets were deplastified in 1-acetoxy-2-methoxyethane (Sigma) for 30 min, rehydrated, DeCal (BioGenex Lab, Fremont, CA) and heat treated, blocked, and subjected to immunofluorescence detection of COL2 or COL10 (for detecting hypertrophic chondrocytes). Primary antibodies were rabbit anti-COL1 antibody (#NB600-408) and biotinylated goat anti-COL2 antibody (#NBP1-26546) from Novus Biologicals (Littleton, CO), and rabbit anti-human Ki67 antibody (#AB66155) and rabbit anti-COL10 antibody (#AB58632) from Abcam (Cambridge, MA). Secondary reagents were goat anti-rabbit IgG-AlexaFluor488 (#A11034) and streptavidin-AlexaFluor594 (#S11227) from Molecular Probes (Eugene, OR). The slides were washed in PBS and mounted with ProLong Gold anti-fade mounting media (Molecular Probes). The % $Ki67^+$ nuclei/$DAPI^+$ nuclei of the $COL2^+$ area was calculated as the average ratio between the number of $Ki67^+$ nuclei and that of ($DAPI^+$) nuclei counted from 3-4 different $COL2^+$ areas per section and multiplied by 100.

Flow Cytometry.

FACS analysis was performed on LSR II (BD). Cell sorting was done with FACS Aria II (BD) as described (Umeda et al., 2015; Umeda et al., 2012). Viable single cells were gated using DAPI (Sigma). Sorted cells ranged in purity from 90 to 95%.

Statistical Analysis.

Statistical differences between groups were determined by Student's t-test (2 categories) or 1-way ANOVA (>2 categories) followed by the Student-Newman-Keuls multiple comparisons by KaleidaGraph (Synergy, Reading, PA) software. n = number of independent experiments.

*: $P<0.1$, **: $P<0.05$, ***: $P<0.01$. $P<0.05$ is considered to be statistically significant, and $P<0.1$ is weakly significant.

4. SUPPLEMENTAL REFERENCES

Burkhardt, M., Glazova, M., Gambaryan, S., Vollkommer, T., Butt, E., Bader, B., Heermeier, K., Lincoln, T.M., Walter, U., and Palmetshofer, A. (2000). KT5823 inhibits cGMP-dependent protein kinase activity in vitro but not in intact human platelets and rat mesangial cells. J Biol Chem *275*, 33536-33541.

Centola, M., Abbruzzese, F., Scotti, C., Barbero, A., Vadala, G., Denaro, V., Martin, I., Trombetta, M., Rainer, A., and Marsano, A. (2013). Scaffold-based delivery of a clinically relevant anti-angiogenic drug promotes the formation of in vivo stable cartilage. Tissue Eng Part A *19*, 1960-1971.

Christensen, A.E., Selheim, F., de Rooij, J., Dremier, S., Schwede, F., Dao, K.K., Martinez, A., Maenhaut, C., Bos, J.L., Genieser, H.G.*, et al.* (2003). cAMP analog mapping of Epac1 and cAMP kinase. Discriminating analogs demonstrate that Epac and cAMP kinase act synergistically to promote PC-12 cell neurite extension. J Biol Chem *278*, 35394-35402.

Gonsalves, F.C., Klein, K., Carson, B.B., Katz, S., Ekas, L.A., Evans, S., Nagourney, R., Cardozo, T., Brown, A.M., and DasGupta, R. (2011). An RNAi-based chemical genetic screen identifies three small-molecule inhibitors of the Wnt/wingless signaling pathway. Proc Natl Acad Sci U S A *108*, 5954-5963.

Langmead, B., and Salzberg, S.L. (2012). Fast gapped-read alignment with Bowtie 2. Nat Methods *9*, 357-359.

Love, M.I., Huber, W., and Anders, S. (2014). Moderated estimation of fold change and dispersion for RNA-seq data with DESeq2. Genome Biol *15*, 550.

Minami, I., Yamada, K., Otsuji, T.G., Yamamoto, T., Shen, Y., Otsuka, S., Kadota, S., Morone, N., Barve, M., Asai, Y.*, et al.* (2012). A small molecule that promotes cardiac differentiation of human pluripotent stem cells under defined, cytokine- and xeno-free conditions. Cell Rep *2*, 1448-1460.

Nakayama, N., Lee, J., and Chiu, L. (2000). Vascular endothelial growth factor synergistically enhances bone morphogenetic protein-4-dependent lymphohematopoietic cell generation from embryonic stem cells in vitro. Blood *95*, 2275-2283.

Pelttari, K., Pippenger, B., Mumme, M., Feliciano, S., Scotti, C., Mainil-Varlet, P., Procino, A., von Rechenberg, B., Schwamborn, T., Jakob, M.*, et al.* (2014). Adult human neural crest-derived cells for articular cartilage repair. Sci Transl Med *6*, 251ra119.

Poppe, H., Rybalkin, S.D., Rehmann, H., Hinds, T.R., Tang, X.B., Christensen, A.E., Schwede, F., Genieser, H.G., Bos, J.L., Doskeland, S.O.*, et al.* (2008). Cyclic nucleotide analogs as probes of signaling pathways. Nat Methods *5*, 277-278.

Proffitt, K.D., Madan, B., Ke, Z., Pendharkar, V., Ding, L., Lee, M.A., Hannoush, R.N., and Virshup, D.M. (2013). Pharmacological inhibition of the Wnt acyltransferase PORCN prevents growth of WNT-driven mammary cancer. Cancer Res *73*, 502-507.

Takamatsu, A., Ohkawara, B., Ito, M., Masuda, A., Sakai, T., Ishiguro, N., and Ohno, K. (2014). Verapamil protects against cartilage degradation in osteoarthritis by inhibiting Wnt/beta-catenin signaling. PLoS One *9*, e92699.

Umeda, K., Oda, H., Yan, Q., Matthias, N., Zhao, J., Davis, B.R., and Nakayama, N. (2015). Long-Term Expandable SOX9(+) Chondrogenic Ectomesenchymal Cells from Human Pluripotent Stem Cells. Stem Cell Reports *4*, 712-726.

Umeda, K., Zhao, J., Simmons, P., Stanley, E., Elefanty, A., and Nakayama, N. (2012). Human chondrogenic paraxial mesoderm, directed specification and prospective isolation from pluripotent stem cells. Sci Rep *2*, 455.

Wang, Y., and Nakayama, N. (2009). WNT and BMP signaling are both required for hematopoietic cell development from human ES cells. Stem Cell Res *3*, 113-125.

Wang, Y., Umeda, K., and Nakayama, N. (2010). Collaboration between WNT and BMP signaling promotes hemoangiogenic cell development from human fibroblast-derived iPS cells. Stem Cell Res *4*, 223-231.